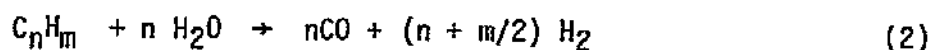
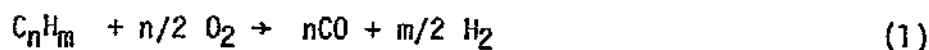


PART I

**AUTOTHERMAL REFORMING OF SULFUR-FREE
AND SULFUR-CONTAINING HYDROCARBON LIQUIDS**

INTRODUCTION

Autothermal reforming (ATR) offers an advantageous alternative to steam reforming for hydrogen production for fuel cells because of the wider range of fuels that can be converted. This process involves the combination of partial oxidation and steam reforming of a hydrocarbon fuel to produce principally hydrogen and carbon monoxide as described in the following reactions:



These reactions are followed by establishment of the equilibria:



Other than reactants' preheat, no external heat source is required since the exothermic reaction 1 plus the preheat sustain the endothermic reaction 2.

In this work, the autothermal reforming of hydrocarbon liquids has been considered as a viable route for hydrogen generation for fuel cell power plants. The particular advantage that this process offers is to expand the range of applicable fuels to heavier petroleum-based and coal-derived liquids. In comparison, light naphtha is the heaviest fuel that can be converted to hydrogen without carbon deposition by conventional steam reforming, which is the process to

be used initially for fuel cells. The applications considered here demand a process with high thermal efficiency, carbon-free operation, and high hydrocarbon conversion efficiency as dictated by equilibrium. Partial oxidation alone has lower thermal efficiency than steam reforming. Carbon formation in this process can be prevented either by increasing the air/fuel ratio (i.e., decreasing thermal efficiency) or by adding steam (1-3), which also increases the hydrogen yield because of simultaneous steam reforming.

The prevention of carbon formation in the catalyst bed is one of the most important aspects of reformer operation. The following carbon producing reactions are possible:



Under certain conditions in the mixture of CO, CO₂, H₂, CH₄ and H₂O, free carbon is thermodynamically possible. This carbon, produced according to reactions 5 and 6, is usually referred to as thermodynamic carbon or Boudouard carbon. Carbon can also be formed as a result of thermocracking of the fuel hydrocarbon used; the olefinic compounds formed degrade to carbon very easily giving an overall reaction as set out in reaction 8.

Using the principle of thermodynamic equilibrium, it is possible to specify which chemical species will be present in the product gases of the autothermal reformer at equilibrium. The computer program used here (4) is based on the minimization of the Gibb's free energy of the system (using graphite data for carbon), and is run under constant system enthalpy, H, and pressure, P, i.e.,

truly adiabatic conditions. In all calculations, a pressure of 1 atm was considered, as this was approximately the pressure in the reactor system in our tests. Also, in the well insulated experimental reactor, a nearly adiabatic operation was achieved.

The autothermal reformer is envisioned as a fuel processor that may have to operate with sulfur in the process stream, because the sulfur compounds (principally thiophenic) in distillate fuel oils are not readily removed by the commonly used desulfurization methods for natural gas and naphtha. By combusting a portion of fuel inside the catalyst bed, higher catalyst temperatures (1200°-1400°K) can be reached than in conventional steam reformers. At these higher temperatures, the supported nickel catalysts commercially used for steam hydrocarbon reforming are anticipated to be less susceptible to sulfur poisoning because of reduced stability of the nickel sulfides (as predicted by thermodynamics (5)). The sulfur content of a fuel may also change the conditions for carbon formation on a given steam reforming catalyst. Hence, particular emphasis was necessary in delineating this possible sulfur-carbon formation relation by well planned experiments.

In a recent JPL report to EPRI (6) on autothermal reforming of No.2 fuel oil, the conditions under which carbon formation started were shown to be much milder than those predicted by the equilibrium theory. Experimental results by other workers (7-9) are in agreement with the JPL data. Follow-on autothermal reforming work at JPL has focused on identifying the causes for the observed behavior of No.2 fuel oil. During this work, tasks have been directed toward delineating the conversion characteristics of individual fuel components

(paraffins, aromatics, olefins, and sulfur compounds) in the autothermal reformer. Since heavy distillate fuels are comprised of a mixture of different hydrocarbons covering a range of boiling points from about 350 to 650°K, the autothermal reforming of both light and heavy compounds was studied. The same catalyst types and configuration as in earlier tests with No.2 fuel oil were used in these tests. Experimental results have been published (10-12) on the ATR of model light and heavy paraffins (n-hexane, n-tetradecane) and aromatics (benzene, naphthalene). These results have demonstrated that differences in chemical reactivity and carbon-forming tendency in ATR are related to the type of fuel hydrocarbon used. Locations and types of carbon in the autothermal reformer have been correlated with intermediate reaction species for each hydrocarbon type. In addition, the effects of the operating parameters on reaction temperature and products, and carbon-forming tendency have been established.

In this report, the previously obtained information on carbon formation from individual paraffins and aromatics is summarized to facilitate comparisons with data collected in the present phase of the experimental ATR work. New experimental results reported herein are from three recent tasks:

(a) Addition of Propylene to Benzene.

In these experiments, the influence of an olefin (propylene) on the ATR characteristics (conversion, carbon formation) of benzene was studied by injecting propylene at different catalyst bed locations.

(b) ATR of Mixtures of Paraffins and Aromatics.

These tests were performed with different mixtures of n-tetradecane and benzene. Using similar operating conditions to those used for the pure mixture components, data were collected on the carbon formation characteristics of these mixtures.

(c) ATR of Sulfur-containing Paraffins and Aromatics.

Thiophene, a good model sulfur compound for heavy distillate fuels was used in these tests in mixtures with either n-tetradecane or benzene to study the conversion and degradation effects of fuel sulfur on the catalyst. Reaction temperatures and products from the ATR of thiophene-contaminated n-tetradecane, and benzene are compared to those pertaining to each pure hydrocarbon. Possible relation between the sulfur content of a fuel and propensity for carbon formation is discussed in view of the experimental data.

EXPERIMENTAL

Apparatus

The design of the autothermal reforming system used in this work has been developed from previous tests with No.2 fuel oil (6) and pure hydrocarbons (10, 11). Figure 1 shows a schematic of the autothermal reformer. During operation, preheated air and steam are mixed first, followed by the injection of vaporized fuel downstream of the mixer. The three components are further mixed in a helical swirler just prior to the reactor entrance. By minimizing the residence time of the fuel inside the mixing tubes in this manner, the extent to which carbon-forming, gas phase reactions proceed is limited and were held to zero in this system. The reactor inlet is made of refractory insulation and has a conical shape to avoid stagnation areas and to provide uniform inlet conditions. Externally, the reactor and all feed lines are insulated to minimize heat losses.

The reactor (3.75 in. I.D.), made from Inconel, was filled to the top flange with catalyst pellets. The catalyst bed configuration is depicted in Figure 1. Off-center, axial bed temperatures were recorded by a chromel-alumel thermocouple probe which traversed inside an Inconel thermowell. A traversing Inconel gas probe was used to sample gaseous reaction products throughout the catalyst bed length. This probe was freely moving inside an Inconel tube which was closed at the end and perforated at 2 in. intervals. Gas samples were analyzed by on-line gas analyzers for H_2 , CO, and CO_2 , and with two gas chromatographs, one with a Flame Ionization Detector (FID) for hydrocarbons, and one with a Flame Photometric Detector (FPD) for sulfur compounds. Pressures and pressure differentials were monitored by pressure transducers, gauges, and manometers.

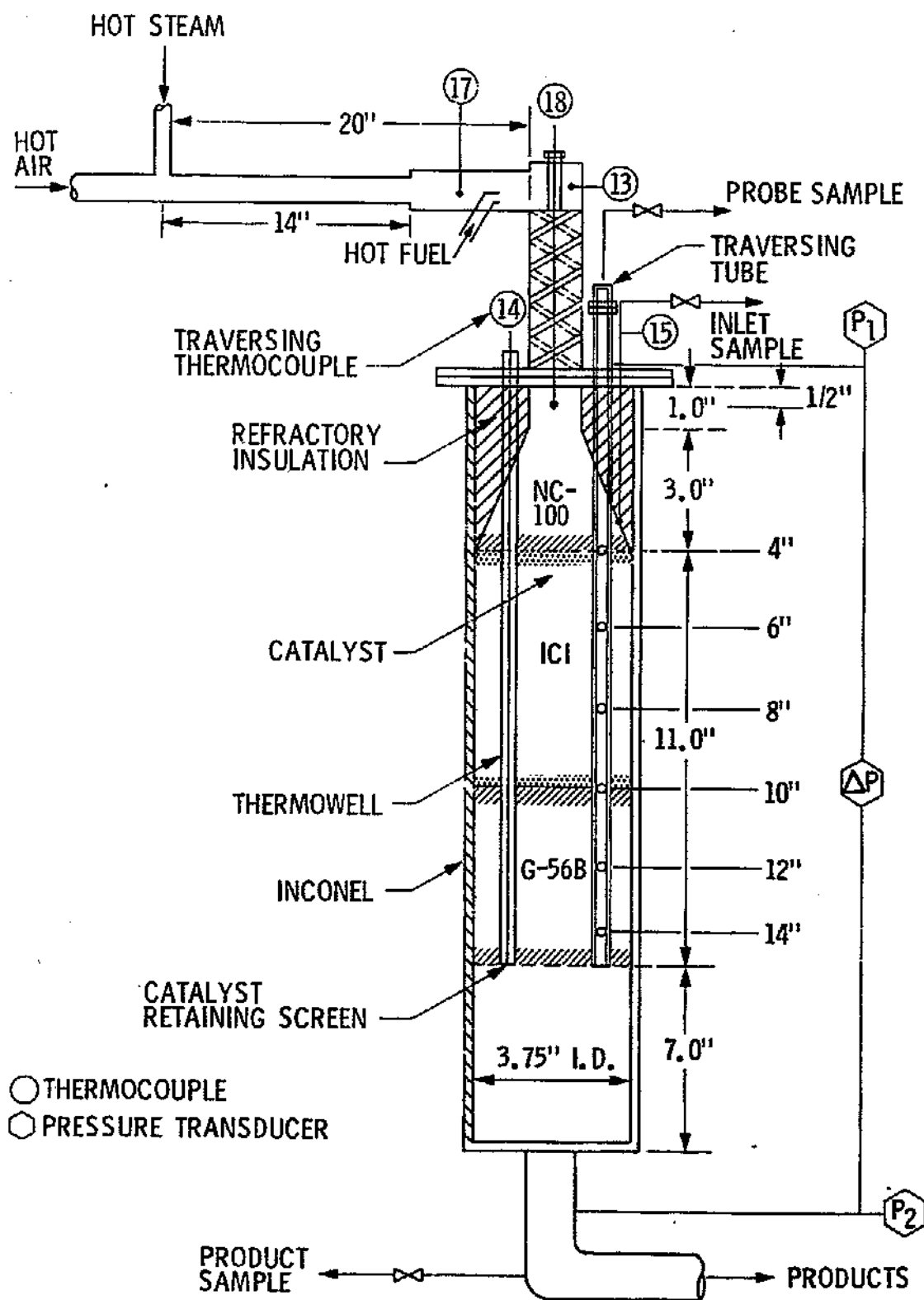


Figure 1. Schematic of the Autothermal Reformer.

Materials

- (a) Fuels. Technical grade n-tetradecane, and pure grade benzene liquids were used in these tests. The technical grade n-tetradecane (Humphrey Chem. Co.) consisted of 100% paraffins, with n-dodecane, branched hexadecane, and branched tetradecane as the only trace impurities. The pure grade benzene (Phillips Chem. Co.) consisted of 99.5 vol.% benzene, and 0.4% other aromatics. The propylene gas (99% +) used as a fuel additive was purchased from Matheson Co. High purity (99% +) liquid thiophene was purchased from Eastman Kodak Co.
- (b) Catalysts. The autothermal reactor was packed with three layers of supported nickel catalysts as shown in Figure 1. In all tests, the top and bottom zones consisted of Norton NC-100 spheres and cylindrical G-56B tablets, respectively. The middle zone was packed either with ICI 46-1 or ICI 46-4 Raschig rings. The physical and chemical characteristics of these catalysts, commercially used in steam reformers, are given in Table I.

The catalyst types and configuration used here were those found to be most effective in previous ATR tests with No. 2 fuel oil (6). The choice of catalyst was dictated by the requirements for enhancing ATR operation, and commercial availability. Thus, in the first zone a low activity catalyst was used to effect a gradual increase in the reactants' temperature to the level of subsequent main reaction temperature, and inhibit carbon formation. The mechanism of heat transfer in this segment is mainly radiation and conduction aided by some exothermal reaction. The Norton NC-100 catalyst spheres were selected to mediate the initial

TABLE I

PHYSICAL AND CHEMICAL CHARACTERISTICS OF TEST CATALYSTS

TRADE NAME	NORTON NC-100	ICI 46-1	ICI 46-4	GIRDLER G-56B
Particle Size, inches	1/2 spheres	11/16 OD x 1/4 ID x 5/16 length	11/16 OD x 1/4 ID x 5/16 length	1/8 x 1/8 cylinders
Bulk (packing) Density, lb/cu ft.	65	72	62	90
Chemical Analysis, wt. %*				
NiO	6.4 - 7.6	21.0	11.0	30.8
SiO ₂	-	14.0	-	0.9
Al ₂ O ₃	-	29.0	77.0	59.9
ZrO ₂	~93.0	-	0.3	-
K ₂ O	-	7.0	-	-
MgO	-	13.0	-	7.0
CaCO ₃	-	-	-	-
CaO	-	13.0	12.0	-
Fe ₂ O ₃	-	3.0	-	-
Fusion Temperature, °F	2650	>2000	>2000	2500
Surface Area, m ² /g	1.0	11.0	14.0	13.0

*Composition as provided by manufacturer

oxidation reaction and help to inhibit precombustion as well as to act as a reactant distributor. These highly porous spheres fill the conical inlet portion of the bed to the top flange as shown in Figure 1, eliminating voids that enhance the probability of precombustion. In the middle zone, an active catalyst capable of oxidizing the hydrocarbons must be used. In this section the oxygen is completely reacted and limited steam reforming is also maintained. The ICI 46-1 catalyst, which contains potassium as a soot-suppressant, was chosen initially in order to reduce carbon formation during steam reforming. This catalyst is in the form of Raschig rings with a high void-to-surface ratio that allows for gas expansion in this region where the initial rapid reaction and temperature rise take place. In experiments with aromatics, the middle zone was filled with ICI 46-4 Raschig rings that have geometry identical to 46-1 but lower nickel loading. This catalyst was used to mediate the high heat release from the aromatic ring oxidation reaction. Finally, the bottom layer of the catalyst bed should contain a highly active, steam reforming catalyst to convert the residual hydrocarbons and methane. In this zone, the Girdler G-56B catalyst was used in the form of small cylindrical pellets. As shown in Table I, these pellets had the highest nickel loading.

RESULTS AND DISCUSSION

All autothermal reforming tests were run at atmospheric pressure and at moderately high reactant preheat temperature, T_p , within the range of 1000-1150°F (800-900°K). This is the temperature recorded by thermocouple No.13 of Figure 1. At each condition, the gas hourly space velocity (G.H.S.V. or S.V. for brevity) was specified. This quantity is defined here as the volumetric flow rate of reactants (NTP) divided by the volume of catalyst corrected for void fraction.

For each fuel, the carbon formation limit was sought as a function of the steam-to-carbon, $(S/C)_m$, and oxygen-to-carbon,* $(O_2/C)_m$, molar ratios at constant pressure and preheat temperature, and over a narrow range of space velocities. The $(O_2/C)_m$, $(S/C)_m$ ratios are defined here as ratios of moles of oxygen and steam respectively to atoms of carbon in fuel based on hourly flow rates. At each $(O_2/C)_m$ ratio, the $(S/C)_m$ ratio was reduced stepwise until carbon began to form with each condition maintained at a steady state for 4 to 6 hours. The determination of carbon formation was detected by a continuous rise in the bed differential pressure and (or) carbonaceous deposits (soot) on the filter in the exhaust product sample line. These "accelerated" carbon formation tests may not describe the precise conditions necessary to completely inhibit carbon for extended periods of reaction. Thus, "carbon formation" is defined here as carbon forming at a rate significant enough to be measured in the time frame during which these tests were conducted.

* To be consistent with the majority of the reported fuel cell work, the oxygen-to-carbon ratio is used here instead of the previously used air-to-carbon, $(A/C)_m$, molar ratio. To convert from $(O_2/C)_m$ to $(A/C)_m$ multiply the former by 4.773.

(A) Summary Of Previous ATR Work With Pure Paraffinic
And Aromatic Hydrocarbons

Carbon Formation in ATR

Experimental results from autothermal reforming tests with several paraffinic and aromatic hydrocarbon liquids have recently been reported (10-12). These have shown clearly that reactive differences exist between these two types of hydrocarbons which affect their carbon formation characteristics in the auto-thermal reformer.

Carbon formation lines were determined experimentally for each fuel at similar operating conditions. These lines separate the carbon-free from the carbon-forming region in the $(O_2/C)_m - (S/C)_m$ plane, i.e., they are the loci of the minimum $(S/C)_m$ ratio before carbon formation begins for a given set of the other operating parameters. In each case, the experimental carbon line was compared to the theoretical one predicted by thermodynamic equilibrium (graphite free energies). The shape of the experimental carbon formation curves was found to be similar for light and heavy hydrocarbons of the same type. However, the heavy homologs of each series formed carbon in ATR at milder conditions than the light ones.

Unique carbon formation characteristics pertaining to each hydrocarbon type were identified indicating different sensitivity to the operating parameters, and possibly different carbon formation mechanisms. Typical carbon formation lines for paraffins and aromatics are shown in Figures 2 and 3, respectively. For n-tetradecane, Figure 2, the experimental carbon formation line converges to the equilibrium line at high $(O_2/C)_m$ ratios, but diverges from it for

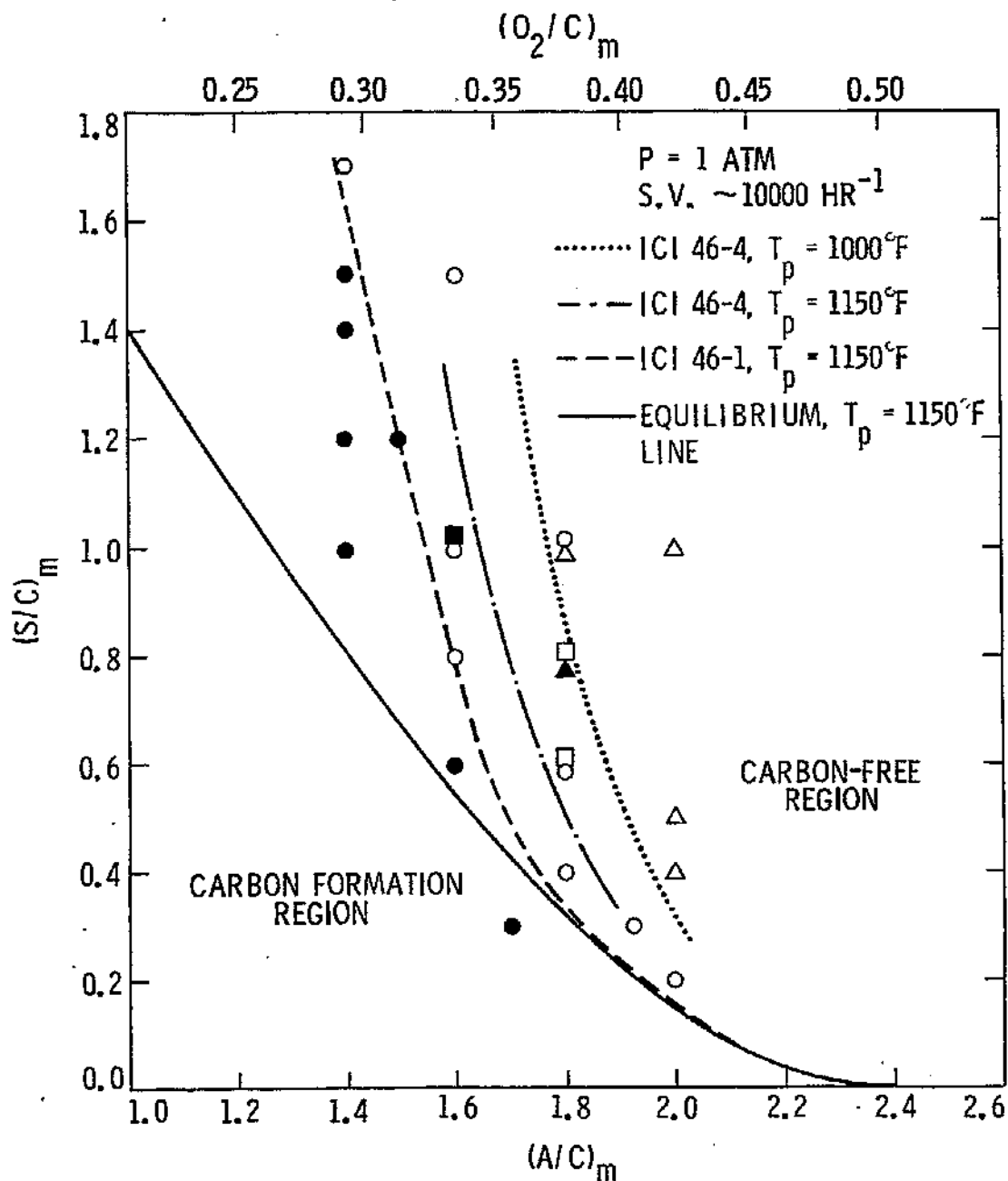


Figure 2. Autothermal Reforming of n-Tetradecane.

Carbon Formation Lines.

Δ, \blacktriangle : ICI 46-4 at $T_p = 1000^\circ\text{F}$.

\square, \blacksquare : ICI 46-4 at $T_p = 1150^\circ\text{F}$.

\circ, \bullet : ICI 46-1 at $T_p = 1150^\circ\text{F}$.

Open Symbols: Carbon-Free

Closed Symbols: Carbon Formation

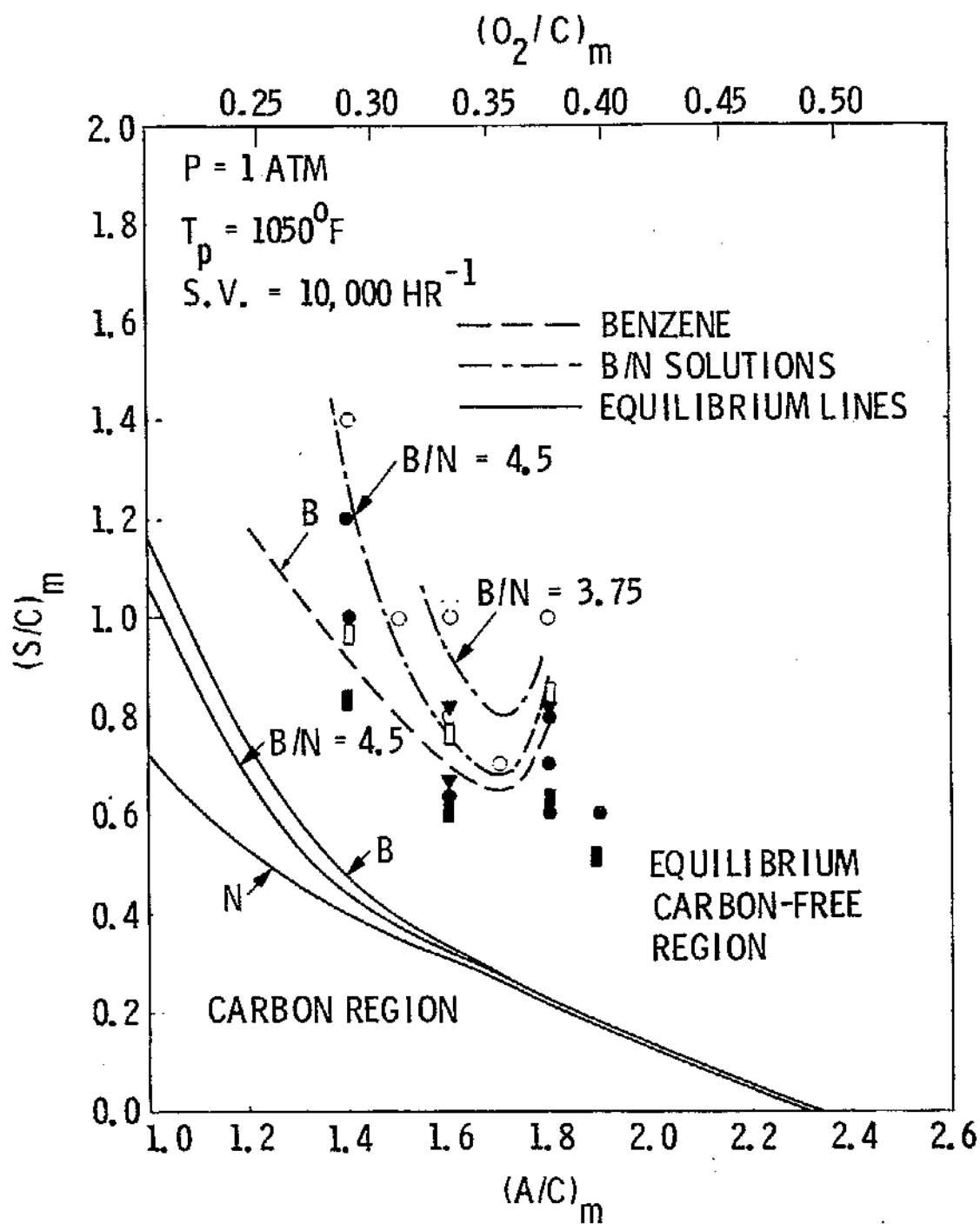


Figure 3. Autothermal Reforming of Benzene and Benzene Solutions of Naphthalene. Carbon Formation Lines.

■: Benzene neat

○●: Benzene/Naphthalene Solution, $(B/N)_m = 4.5$

▽▼: Benzene/Naphthalene Solution, $(B/N)_m = 3.75$

Open Symbols: Carbon-Free

Closed Symbols: Carbon Formation

$(O_2/C)_m$ values lower than about 0.33. On the other hand, the carbon formation lines for benzene, and benzene solutions of naphthalene, Figure 3, diverge from equilibrium at high $(O_2/C)_m$ ratios, and are almost parallel to the theoretical lines at low $(O_2/C)_m$ ratios, thus exhibiting a minimum. This minimum $(S/C)_m$ value occurs at $(O_2/C)_m$ of about 0.36, and is a unique characteristic of the behavior of aromatics in ATR.

The effect of different reactant preheat temperatures on carbon formation is depicted in Figure 2 for the ATR of n-tetradecane. The dotted and hatched curves in this figure were determined on the same catalyst (with ICI 46-4 in the middle zone) for $T_p = 1000^\circ F$ ($811^\circ K$) and $1150^\circ F$ ($894^\circ K$), respectively. The carbon forming tendency was higher at lower reactant preheat temperatures. The effect of different catalyst types in the middle reactor zone is shown for n-tetradecane by the hatched and dashed curves of Figure 2. For the same preheat temperature of $1150^\circ F$ ($894^\circ K$), the experimental carbon line corresponding to ICI 46-1 catalyst is located closer to the equilibrium line than for ICI 46-4, which does not contain potassium oxide as a soot-suppressant.

Potential carbon precursors for each hydrocarbon type in ATR were sought in comparative studies of axial bed temperature and reaction profiles. Both carbon-free and carbon-forming conditions were examined. Figures 4 and 5 show typical plots of axial bed temperatures and gas compositions, respectively, for benzene and n-tetradecane run under the same autothermal reforming operating conditions (carbon-forming). Bed temperature profiles are very different for the two hydrocarbons, while reaction intermediates throughout the bed differ in amounts only, not in type. The experimental results plotted in Figures 4 and 5 indicate the following:

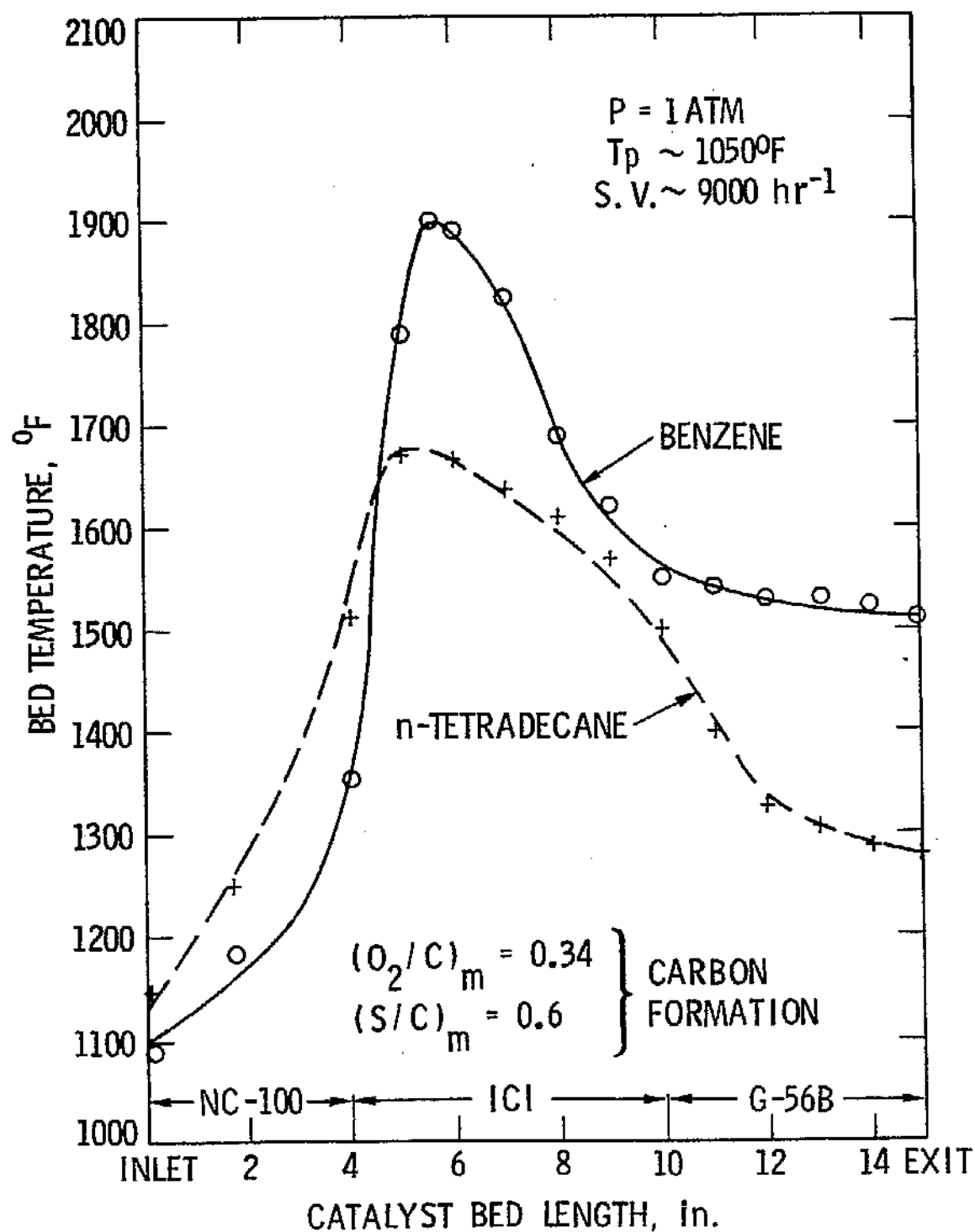


Figure 4. Axial Bed Temperature Profiles.
 — ATR of n-Tetradecane, ICI 46-1
 — ATR of Benzene, ICI 46-4.

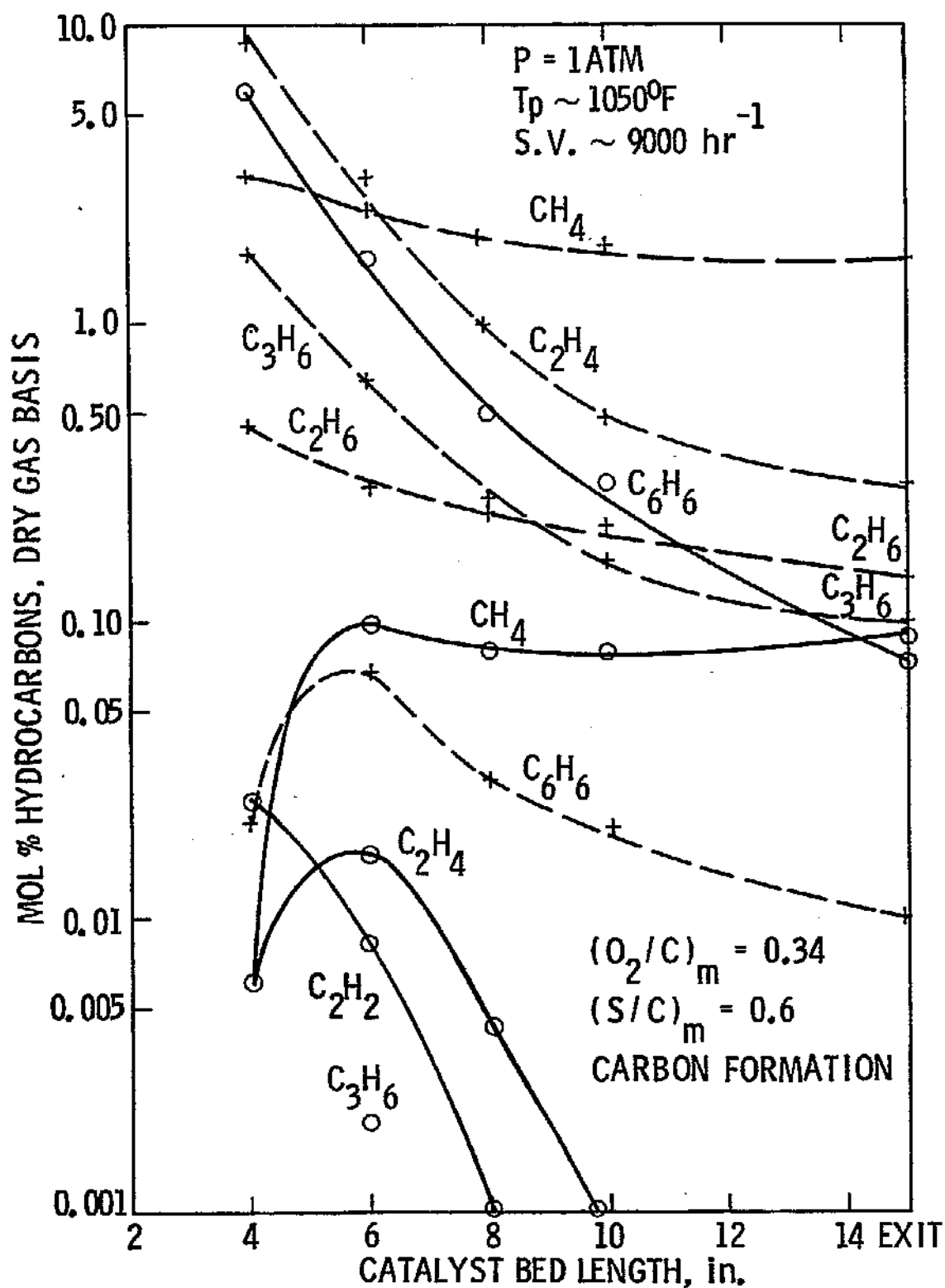


Figure 5. Axial Bed Composition Profiles.
 --- ATR of n-Tetradecane, ICI 46-1
 — ATR of Benzene, ICI 46-4

- (a) Two main reaction zones exist for aromatics. The first, partial oxidation of the fuel, takes place in a very narrow region well downstream of the reactor inlet. This is depicted by sharp-peaked axial bed temperature profiles with zero initial slope. A complete absence of benzene cracking (to olefins and acetylenes) at the inlet, and very limited reaction in the top catalyst zone account for the slopes of the ascending portion of the temperature profile, and the higher bed temperatures compared to *n*-tetradecane. In the immediate vicinity of the temperature peak, hydrocarbons such as ethylene, acetylene and methane are rapidly produced and reach a peak. The first two of these intermediate species are indicative of benzene cracking, which however is very limited, as was found by mass balance calculations.

The second reaction zone for aromatics involves the steam reforming reaction, which mainly begins upon completion of the first reaction (partial oxidation), initially at high temperatures, and then at lower temperatures in the lower half of the catalyst bed. The slopes of the descending (past the temperature peak) portion of the temperature profile for benzene in Figure 4 indicate that steam reforming occurs at a fast rate close to the temperature peak (large slope), but it is limited in the last catalyst zone, where the temperature profile levels off. From Figure 5, we can see that the profiles of unconverted benzene and produced methane are commensurate with temperature changes in this catalyst zone. Thus, the slope of the unconverted benzene profile is decreasing through the length of the bed downstream of the temperature peak, while that of methane is almost constant in this region, and slightly increasing towards the reformer exit. On the other hand, cracking products

disappear rapidly and are no longer detected in gas samples taken from the lower end of the bed. Since carbon is being formed throughout the steam reforming region of the bed (see below), and because the olefins and acetylene are negligible in the gas phase throughout the bed, the main carbon precursor appears to be the aromatic molecule (benzene) itself. Benzene may form carbon through dehydrogenation in the gas phase at the high temperatures prevailing in the vicinity of the temperature peak. The rate of carbon formation by this mechanism may exceed the rate of carbon removal by gasification for a given range of temperature and limited steam availability. Further down the bed, at lower temperature, surface-bound carbon may be produced from benzene-nickel interaction. The fact that the methane concentration did not decrease through the lower part of the bed seemed to be unrelated to carbon formation, since it was also observed under carbon-free conditions.

- (b) In the case of paraffins, the same two reaction zones were identified as for the aromatics, i.e., partial oxidation and steam reforming. However, a third zone, cracking to low molecular weight olefins and paraffins, was very pronounced in the top part of the catalyst bed. This is portrayed by the temperature and reaction profiles of Figures 4 and 5. These intermediate cracking products were already detectable at the bed inlet (up to 25 vol.% of the incoming n-tetradecane cracks at the inlet (10)), and peaked just upstream of the temperature peak location. In addition, a small amount of benzene was produced in the upper part of the bed indicative of cyclization reactions. The benzene profile also peaked just prior to the temperature peak. Because of the endothermic cracking reactions, bed temperatures were lower for n-tetradecane than for benzene.

Partial oxidation was taking place throughout the front end of the bed in the case of n-tetradecane (paraffins being much less refractory than aromatics), as indicated by larger initial slope of the n-tetradecane temperature profile.

Similar to the aromatics, the continuous drop in bed temperature begins immediately past the temperature peak, due to steam reforming of the paraffins and olefins just produced. In the vicinity of the temperature peak, at the prevailing high temperatures, both gas phase and surface carbon formation may take place principally from the olefins abundant in this region of the bed since the benzene intermediate is present in negligible amounts. Figure 5 shows that the profiles of the olefins (and not the paraffins) have the largest slope (highest rate of conversion) in the bed. Close to the bed exit, all species' profiles level off, indicating low steam reforming reaction rates. At the low temperatures of this region, the rate of carbon formation by olefin degradation on the catalyst surface may exceed the rate of carbon removal if there is not enough steam available.

It should be noted that the same reaction intermediates have been detected in ATR either under carbon-free or carbon-forming conditions. The extent of cracking, however, was much higher under carbon-forming conditions, and resulted in lower steam-to-carbon ratios in the region of the bed downstream of the temperature peak. As we have discussed in a previous report (11), the rates of carbon formation are greatly affected by changing the $(S/C)_m$ ratio, more so than by temperature changes. In the following section, the locations for carbon formation in ATR are

shown to be within the steam reforming region of the bed at the operating conditions considered in this work.

Locations and Types of Carbon in ATR

Information about the locations of carbon deposition and types of carbon formed in the catalyst bed was obtained by examination of the bed after carbon-forming conditions, and analyses of catalyst samples by Scanning Electron Microscopy (SEM), Thermal Gravimetric Analysis (TGA) and X-ray Diffraction (XRD).

For both paraffinic and aromatic hydrocarbons, catalyst from the front end of the bed always appeared free of carbon deposits and retained its structural integrity. No surface grown carbon was found on the catalyst in this region where partial oxidation of the fuel mainly occurs. On the other hand, catalyst from the lower half of the bed had an eroded appearance, and broken pieces and fines were collected from this region of the bed where steam reforming takes place. This physical breakdown of the catalyst material can be attributed to carbon formation inside the pores followed by carbon removal (13) during the desooting process. Figures 6a and b show SEM photomicrographs of the upper and lower half, respectively, of ICI 46-1 catalyst used in the ATR of n-tetradecane. Needle-like carbon growths from all directions inside the pores are seen in Figure 6b, while no carbon is seen in Figure 6a at the same magnification. The same catalyst samples were also checked for carbon by TGA, and the results are in agreement with SEM.

Surface grown carbon was identified by SEM on samples from the lower part of the catalyst bed. Figure 7 shows a typical SEM photomicrograph of the surface of the lower end of ICI 46-1 catalyst bed used in ATR of n-tetradecane under

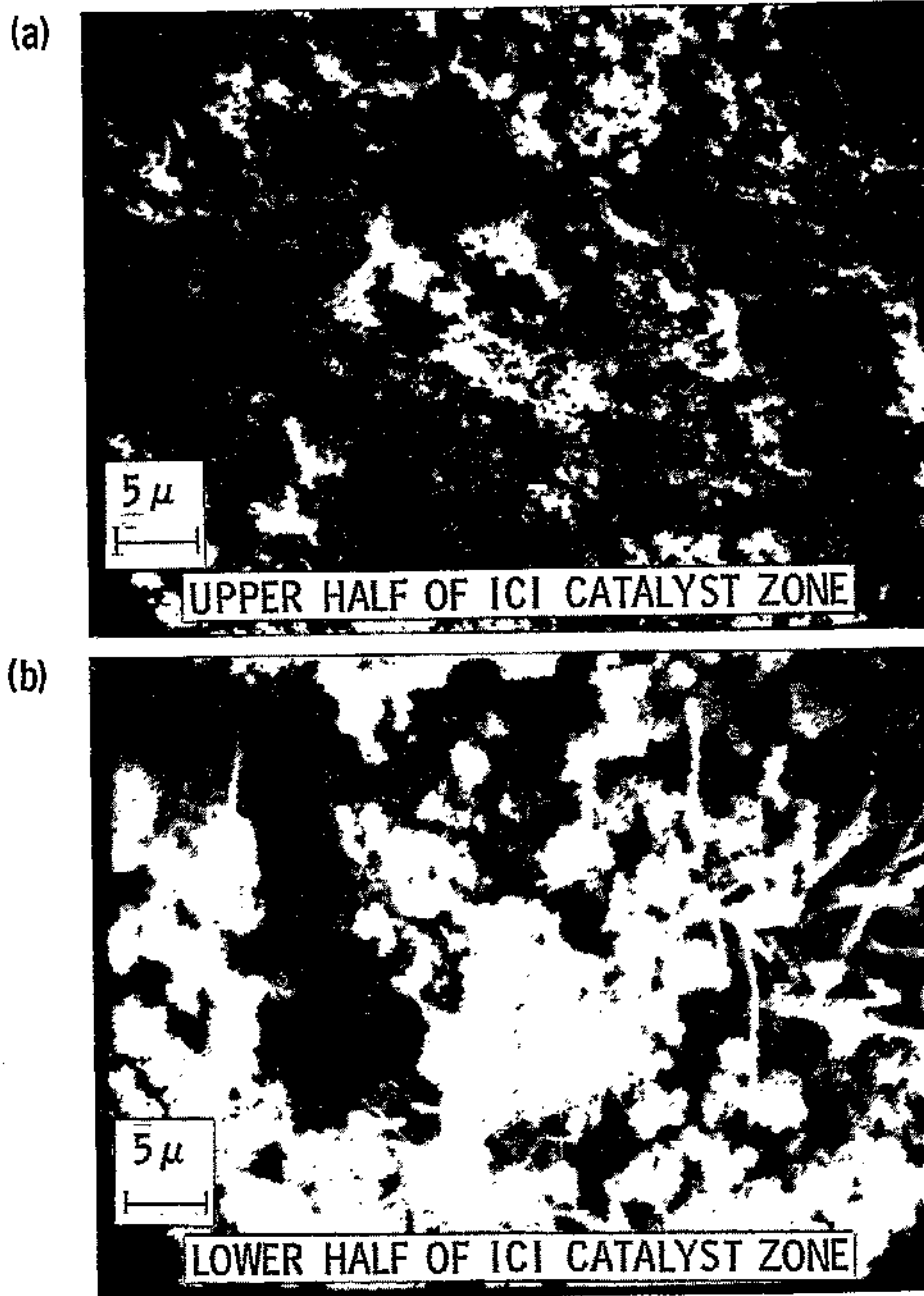


Figure 6. SEM photomicrographs of the surface of ICI 46-1 catalyst used in ATR of n-Tetradecane under carbon-forming conditions: $P = 1 \text{ atm}$, $T_p = 1150^\circ \text{F}$, $(O_2/C)_m = 0.34$, $(S/C)_m = 0.6$, and $S.V. = 10,000 \text{ hr}^{-1}$.

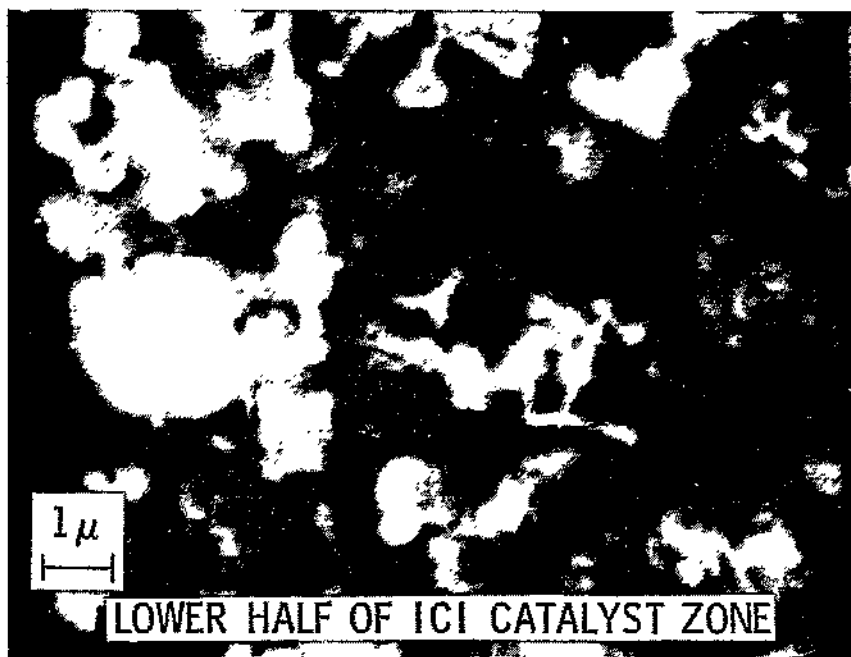


Figure 7. SEM photomicrograph of the surface of ICI 46-1 catalyst used in ATR of n-tetradecane under carbon-forming conditions: $P = 1 \text{ atm}$, $T_p = 1150^\circ\text{F}$, $(\text{O}_2/\text{C})_m = 0.38$, $(\text{S}/\text{C})_m = 0.25$, and $\text{S.V.} = 10,000 \text{ hr}^{-1}$.

carbon-forming conditions. Tubular carbon whiskers are observed that appear to have a nickel crystallite located at the end. The diameter of the whisker is very close to that of the nickel crystallite. These observations are in agreement with earlier reports by Rostrup-Nielsen (14) on coking studies under steam reforming conditions. Further XRD analysis of the catalyst samples that showed evidence of surface grown carbon indicated that graphite carbon was present.

In addition to surface grown carbon, evidence of gas phase carbon formation was obtained from large amounts of soot (carbon fines) collected from the interstices between catalyst particles throughout the lower two thirds of the catalyst bed. Heavy deposits of this type of carbon were found on the catalyst surfaces, but they did not appear to be surface-bound. The gas phase carbon, as found by XRD, consisted of a mixture of amorphous (non-crystalline) and graphitic carbon forms. The locations of gas phase carbon formation cannot be defined with certainty, because carbon fines found in the lower half of the bed could have originated either there or upstream, and transferred down by the flowing gases. It appears that the most probable location for this type of carbon formation is around the temperature peak, where thermocracking of paraffins to olefins, which can easily degrade to carbon, or degradation of aromatics to carbon proceed at the fastest rates.

Differences between the types of carbon produced during the ATR of paraffinic and aromatic hydrocarbons have not been quantified. However, from several examinations of the catalyst bed after operation at carbon-forming conditions, gas phase carbon formation in the middle catalyst zone appeared to be more extensive for aromatics than for paraffins. Limited surface-bound carbon was

detected in the middle catalyst zone in the case of aromatics. Further downstream, in the lower catalyst zone, surface grown carbon was detected with either hydrocarbon type.

These results indicate possible differences in the mechanisms of carbon formation between paraffins and aromatics. As discussed in the previous section, at the high temperatures prevailing in the middle catalyst zone, immediately past the location of complete oxygen consumption (temperature peak), paraffins crack to olefins. These can then degrade to carbon either in the gas phase or on the catalyst/support surface at a rate exceeding that of carbon removal (depending on the conditions). Thus, both types of carbon observed may have olefinic precursors. Aromatics, on the other hand, may form gas phase carbon at these high temperatures by fission of the C-H bonds rather than the C-C bonds. This hypothesis is supported by (a) negligible amounts of reaction intermediates (olefins, acetylenes) from aromatics as compared to considerable amounts of intermediates from cracking of paraffins and (b) the characteristic "minimum" in the experimental carbon formation line for aromatics, whereby an increase in the $(O_2/C)_m$ ratio (i.e., a temperature increase) has an adverse effect on carbon formation, possibly indicating the onset of gas phase benzene dehydrogenation to form carbon at a faster rate than the surface reaction (with steam). Finally, in the lower catalyst zone, where steam reforming takes place at continuously decreasing temperatures, the rates of surface carbon formation from either hydrocarbon type may exceed the steam reforming rates depending on the excess steam and temperature available in this part of the bed. A concise performance comparison of the autothermal reforming paraffins and aromatics is given in Table II. The main characteristics of each hydrocarbon type in ATR, as discussed above, are listed in this table.

TABLE II

ATR PERFORMANCE COMPARISON
OF PARAFFINIC AND AROMATIC HYDROCARBONS

ATR VARIABLES	PARAFFINS	AROMATICS
Inlet Reactions	Extensive cracking	No cracking
Exit Reactions	Steam reforming	Steam reforming slower than paraffins; methanation
Bed Temperature Profiles	Broad-peaked; slow rise and fall	Sharp-peaked; zero slope at inlet and exit of bed
Peak Temperatures	Low	Higher than paraffins
Intermediate Hydrocarbon Species	Predominantly olefinic; low aromatic	Predominantly unconverted aromatic; low olefins, acetylene
Carbon Formation Conditions	Low O_2/C , low S/C ; High molecular weight	High O_2/C , low S/C ; polynuclear aromatics
Carbon Types	Surface carbon growths (whiskers) Gas phase carbon (fines in voids)	Limited surface carbon growths Extensive gas phase carbon formation
Location of Carbon Deposits	Surface carbon } Throughout steam reforming zone Gas phase carbon } Vicinity of temperature peak?	Surface carbon } Throughout steam reforming zone Gas phase carbon } Vicinity of temperature peak?
Catalyst Erosion	Considerable	Less extensive

(B) Addition Of Propylene To Benzene

In this work, a new series of tests with benzene were run in the autothermal reformer in which the effects of olefin addition on reaction products and carbon formation were studied. Propylene, one of the main reaction intermediates in the autothermal reforming of paraffins (10-12) was the olefin used in these tests. The baseline operating conditions with pure benzene were chosen in the carbon-free region. The amount and location of propylene injection into the reformer were varied, thereby permitting the identification of the reaction zone most prone to carbon formation under the chosen operating conditions.

Tests CP-183 through 190 were run in the ATR reactor on the same catalyst bed. This was composed of the usual upper and lower zone catalysts, NC-100 and G-56B, respectively, while in the middle zone the ICI 46-4 catalyst was used. The reactants' preheat temperature, T_p , was kept at 1050°F, and the $(O_2/C)_m$ and $(S/C)_m$ ratios, based on benzene only, were 0.33 and 0.80, respectively. Carbon-free operation for benzene neat was expected for these conditions based on previous data (10), and this was verified in tests CP-183, 184. As can be seen in Figure 3, however, this data point lies close to the experimentally determined carbon formation line for benzene, so that with rather small perturbations on the operating conditions, carbon deposition may take place. Propylene gas was added at various bed locations at flowrates of 0.02, 0.045, 0.20 and 0.40 lb/hr. Because of the low flowrates of propylene added, the space velocity in all runs remained approximately the same at 9500 hr⁻¹.

Table III summarizes the data collected from these runs, and Table III-a shows longitudinal bed temperatures for each test run. Also shown in Table III are baseline data from tests CP-183, 184, which were run with pure benzene without carbon formation. The dry gas product analysis from the pure benzene tests showed a total of 900 ppm hydrocarbons, of which 700 ppm were CH_4 and 200 ppm were unconverted benzene. In tests CP-185 through 187, and in CP-189-1, propylene was injected through the access tube of TC-18 (located 1/2 inch below the reactor inlet, Figure 1) in progressively higher amounts from 0.02 to 0.40 lb/hr. The total hydrocarbon content of the product gases in CP-189-1 (with 0.4 lb/hr propylene addition) was increased to 4500 ppm, of which 4200 ppm was CH_4 and 300 ppm benzene. In all cases, no unconverted propylene was detected in the product gases, and the operation remained carbon-free. As can be seen from Table III-a, bed temperatures were lower when propylene was injected at the inlet of the catalyst bed, mainly because the propylene was added at room temperature, but in part because of changes in the $(\text{O}_2/\text{C})_m$ and $(\text{S}/\text{C})_m$ ratios effected by the propylene addition. Thus, $(\text{O}_2/\text{C})_m$ and $(\text{S}/\text{C})_m$ ratios of 0.33 and 0.80 respectively for 6 lb/hr flow of benzene, became 0.31 and 0.76 respectively upon addition of 0.4 lb/hr propylene.

Following these tests, propylene was injected at eight inches below the reactor inlet using the gas probe access tube. With 0.20 lb/hr propylene addition, test CP-188-1, unconverted propylene was detected in the exhaust gases, but the reactor could still be operated in the carbon-free region. However, when the flowrate of propylene was raised to 0.40 lb/hr, injection at this level led to carbon formation in the bed (tests CP-188-3, 189-2). Carbon was detected by a sooty deposit in the sample line filter. The recorded temperatures in this

TABLE III

AUTOTHERMAL REFORMING OF BENZENE

Effects of Propylene Addition on Conversion

TEST Q -	FUEL	(O ₂ /C) _m	(S/C) _m	T _p	(2) MAX. BED TEMPERATURE		(3) m ³ /hr	(4) S.V.	C A R B O N	(5) GAS PROBE	DRY GAS COMPOSITION, MOL %																																																																																																																																																																																																																																																																																																																																																																																																																																																																																																																																																																																																																																																																																																																																																																																																																																																																																																																																																																																																																																																																																																																																																																																																																																																																																																																																				
					T _{MAX} °F	AT IN.					H ₂	CO ₂	CO	HC _T	CH ₄	C ₂ H ₄	C ₂ H ₆	C ₃ H ₈	C ₄	C ₅	C ₆	C ₆ H ₆																																																																																																																																																																																																																																																																																																																																																																																																																																																																																																																																																																																																																																																																																																																																																																																																																																																																																																																																																																																																																																																																																																																																																																																																																																																																																																																									
							°F	IN.	LB/HR	HR ⁻¹													AT INCHES																																																																																																																																																																																																																																																																																																																																																																																																																																																																																																																																																																																																																																																																																																																																																																																																																																																																																																																																																																																																																																																																																																																																																																																																																																																																																																																								

TABLE III (Cont'd)

TEST	FUEL	(O ₂ /C) _m	(S/C) _m	(1) T _P	(2) MAX. BED TEMPERATURE		(3) m _f	(4) S.V.	C A R B O N	(5) GAS PROBE	DRY GAS COMPOSITION, MOL %														
					°F	T _{MAX} °F					AT IN.	LB/HR	HR ⁻¹	O N	AT INCHES	H ₂	CO ₂	CO	HCT	CH ₄	C ₂ H ₄	C ₂ H ₆	C ₃ H ₈	C ₃ H ₆	C ₄
189-1 ⁺	Benzene +0.4 lb/hr Propylene	0.31 " " " "	0.76 " " " "	1050 " " " "	1645 1644 1648 1645 1661	7.8 7.8 7.8 7.8 7.8	6.40 " " " "	9580 " " " "	NO " " " "	0 4 6 8 EXIT	- 0.99 28.15 32.57 33.35	- 0.97 6.57 6.36 5.35	- 1.92 22.71 23.59 25.39	7.41 7.25 1.34 0.60 0.45	0.01 0.01 0.07 0.09 0.42	- - 0.02 - -	- 0.01 - - -	- 1.06 1.20 0.09 0.02 -	- - - - -	- - - - -	- - - - -	- - - - -	- - - - -	6.34 6.03 1.16 0.49 0.03	
188-1 ⁺⁺	Benzene +0.2 lb/hr Propylene	0.33 [*]	0.80 [*]	"	1734	6.8	6.0 [*]	9500 [*]	NO	EXIT	32.25	6.06	25.19	0.43	0.14	0.01	-	0.23	-	-	-	-	-	-	0.05
188-2	Benzene	0.33	0.80	1050	1715	6.8	6.0	9500	NO	EXIT	32.48	6.43	23.82	0.09	0.07	-	-	-	-	-	-	-	-	-	0.02
188-3 ⁺⁺	Benzene +0.4 lb/hr Propylene	0.33 [*]	0.80 [*]	1050	1725	6.8	6.0 [*]	9500 [*]	YES	EXIT	33.17	5.84	24.31	0.58	0.29	-	-	-	0.21	-	-	-	-	-	0.08

(1) Preheat temperature, T.C. No. 13 (Fig. 1)

(2) Maximum bed temperature and location with reference point at the reactor inlet

(3) Mass flowrate of fuel

(4) Space velocity based on reactants' flowrates (NTP)

(5) Gas sample probe location with reference point at the reactor inlet

TABLE III-a
 AUTO THERMAL REFORMING OF BENZENE
 Effects of Propylene Addition on Bed Temperatures

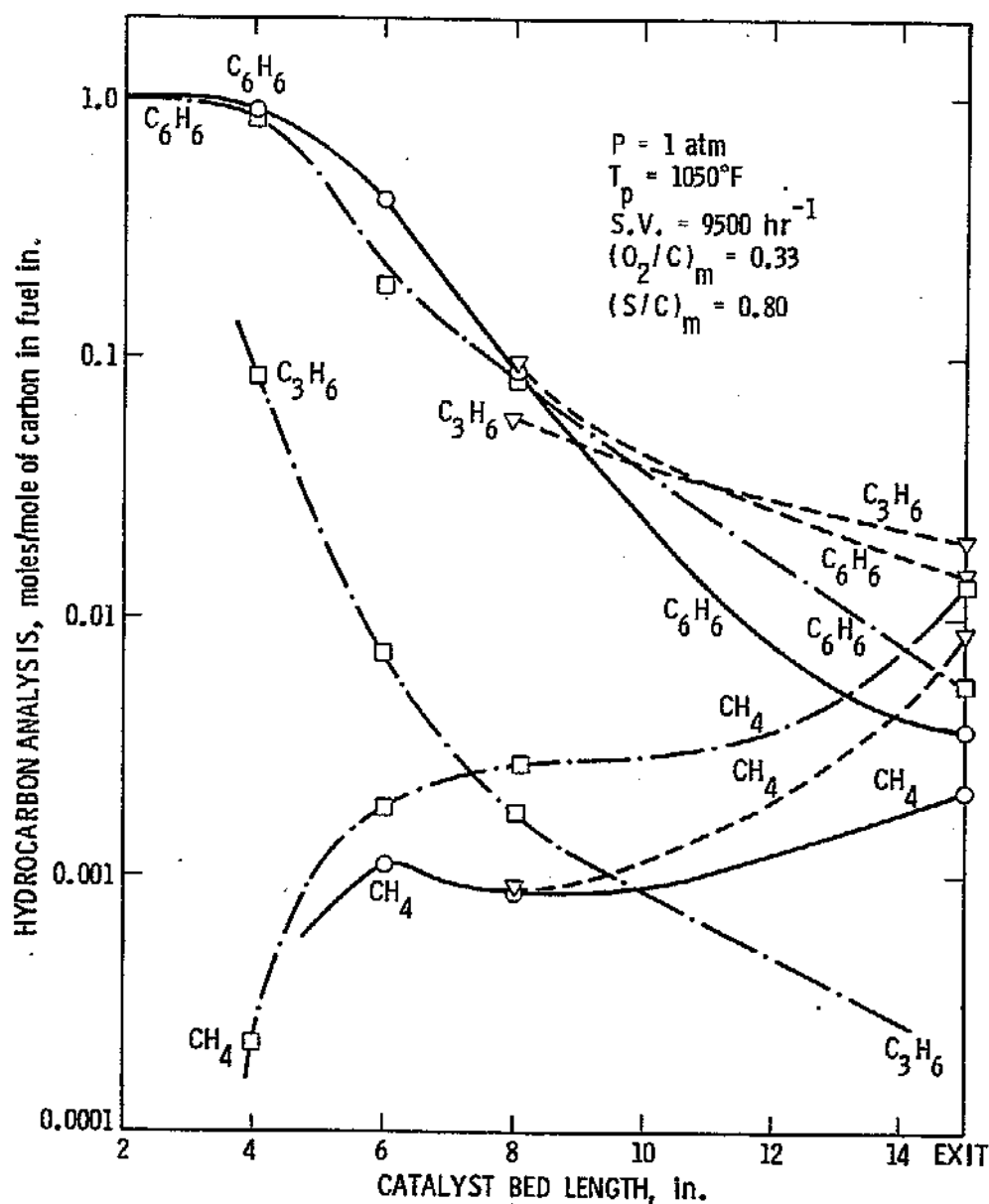
TEST CP -	$(O_2/C)_m$	$(S/C)_m$	(1) T_p °F	S. V. hr ⁻¹	BED TEMPERATURE, °F At (in. from Reactor Inlet)														
					0.5	3	4	5	6	7	8	9	10	11	12	13	14	15	
184	0.33	0.8	1070	19447	1068	1283	1282	1651	1731	1744	1719	1659	1596	1542	1482	1451	1443	1451	
186	0.33	0.8	1061	9447	1060	1277	1270	1632	1750	1757	1743	1688	1624	1572	1520	1496	1488	1487	
188-1	0.33	0.8	1062	9447	1060	1230	1267	1607	1711	1733	1711	1649	1592	1554	1498	1470	1453	1448	
-2	"	"	"	"	1064	1222	1275	1630	1742	1764	1763	1692	1630	1581	1529	1489	1476	1465	
-3	"	"	"	"	1065	1217	1247	1574	1694	1723	1708	1657	1601	1557	1486	1453	1428	1420	
189-1	0.33	0.8	1050	9447	1049	1195	1194	1523	1626	1646	1659	1601	1540	1494	1421	1387	1362	1350	

(1) Preheat Temperature, T.C. No. 13 (Figure 1)

case were higher than those corresponding to injection at the inlet (see Table III-a). However, this did not prevent carbon formation.

These results indicate that olefin (in this case, propylene) addition to the reacting gas mixture in ATR can cause carbon formation, only after a "critical" amount of the olefin has been reached. The important finding of this study is that this "critical" amount of propylene is higher if the injection is made at the reactor inlet rather than at a level 8 inches downstream of the inlet. In other words, higher amounts of propylene can be "tolerated" at the reactor inlet. This means that the relative competition of benzene and propylene for the available oxygen at the front end of the reactor does not produce a carbon formation situation. This was also observed for injection of propylene at other points upstream of the main oxygen depletion zone, which corresponds to the bed temperature peak region. The extent of propylene/benzene-oxygen reaction in this region is sufficient to convert an adequate amount of propylene and generate enough heat to steam reform the ensuing "carbon precursor" hydrocarbon species. The 8 inch injection level, on the other hand, located about 1 inch downstream of the temperature peak for these runs, is in the region where steam reforming, unaided by oxygen, takes place. A reduction in the overall value of the steam-to-carbon ratio at this level can be crucial for carbon formation (11).

Figure 8 shows axial dry gas hydrocarbon profiles for the conditions of tests CP-183, 189-1, and 188-3 corresponding to neat benzene, and benzene + 0.4 lb/hr propylene injected at the inlet and the 8 inch level of the bed, respectively. The propylene content of the mixtures at the 8 inch level was calculated by solving the mass balance equations, which were also used to calculate the



(S/C) _m RATIOS AT THE 8" LEVEL				
TEST	(S/C) _{m, B}	(S/C) _{m, P}	(S/C) _{m, M}	(S/C) _{m, T}
○ CP-183	3.66	-	368	3.62
□ CP-189-1	2.64	132	85	2.50
▽ CP-188-3	3.66	5.41	368	2.17

Figure 8. Addition of Propylene to Benzene. Effect of injection location on axial bed hydrocarbon profiles.

- ATR of C_6H_6 neat, test CP-183.
- - - ATR of C_6H_6 w/ C_3H_6 (inlet injection), test CP-189-1.
- - - ATR of C_6H_6 w/ C_3H_6 (8" level injection), test CP-188-3.

$(S/C)_{m,i}$ ratios (where i = Benzene (B), Propylene (P), Methane (M), or Total Hydrocarbons (T) at this level). The ordinate in Figure 8 gives moles of each species per carbon atom in the fuel at the inlet. The change of slope of the curves of Figure 8 (indicating rate changes) illustrates the effect of propylene addition on benzene conversion and carbon formation. With 0.4 lb/hr propylene injection at the inlet, the benzene conversion is somewhat inhibited, and methane goes up, while propylene disappears faster than benzene. As shown in the bottom of Figure 8, the overall $(S/C)_{m,T}$ ratio at the 8 inch level is 2.5 in this case, lower than the 3.6 value corresponding to the data for neat benzene. However, this ratio is still adequate to steam reform "carbon precursors" that might result from either propylene or benzene, and no carbon is detected either at this level or at the bed exit. With 0.4 lb/hr propylene injection at the 8 inch level, however, the amount of unconverted benzene at the exit is further increased, the rate of propylene conversion is low, and the methane content of the exhaust gases is lower than that required for complete carbon balance. Carbon detected in this case had been formed presumably in the part of the bed downstream of the 8 inch level. The overall $(S/C)_{m,T}$ ratio at this level was calculated to be 2.2, a value not adequate to steam off the carbon formed.

In Figure 9, a comparison similar to that of Figure 8 is depicted for tests CP-183, 188-1, and 188-3 corresponding to neat benzene, and benzene plus 0.2 lb/hr and 0.4 lb/hr, respectively, of propylene. The propylene gas was injected at the 8 inch level in both CP-188-1 and 188-3. No carbon was observed in test CP-188-1 (0.2 lb/hr propylene addition). As can be seen from Figure 9, in the remaining 7 inches of the bed downstream of the injection point the rate of benzene conversion decreases, and the rate of methane formation increases,

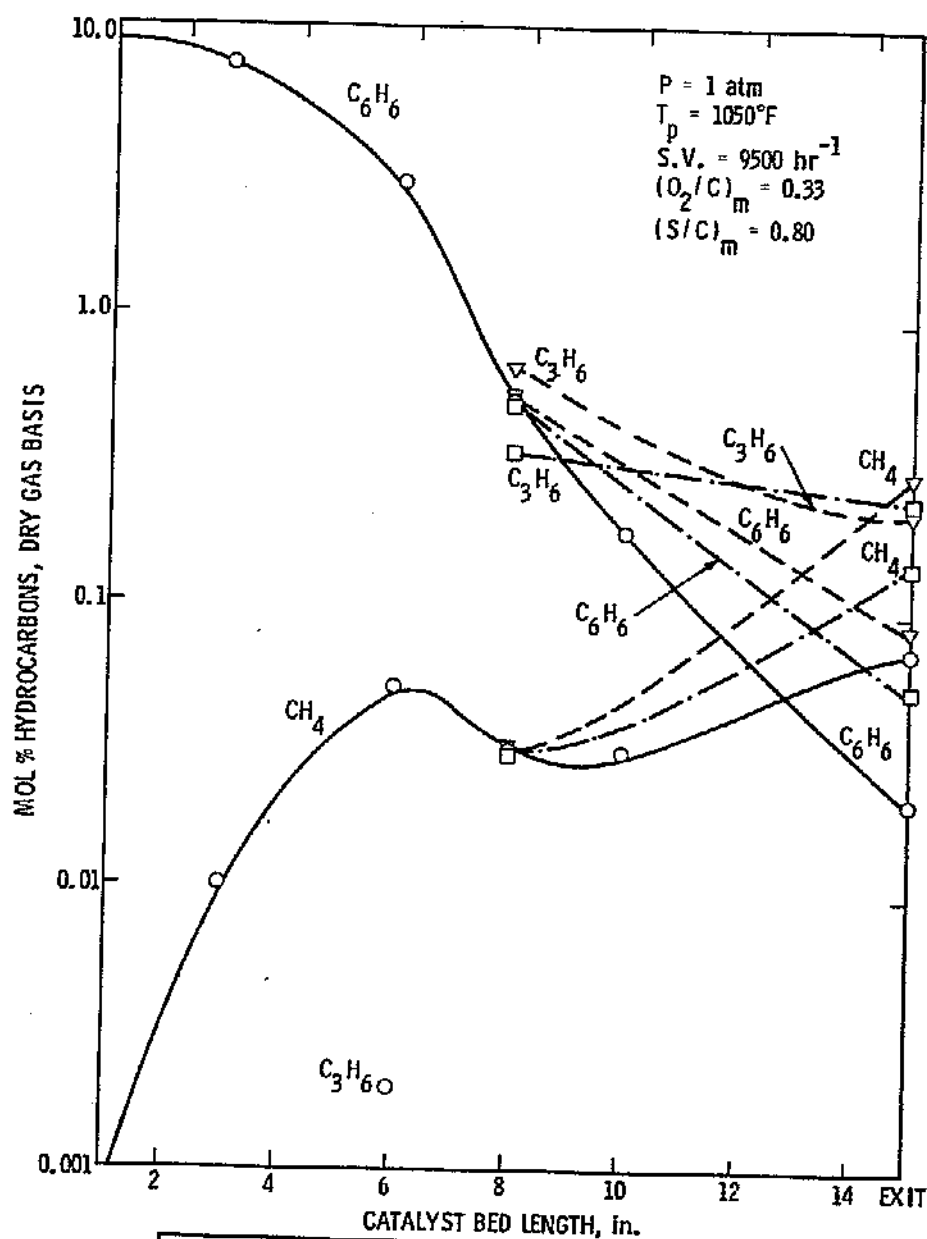


Figure 9. Addition of Propylene to Benzene. Effect of propylene flowrate on axial bed hydrocarbon profiles.

- ATR of C_6H_6 neat, test CP-183.
- - - ATR of C_6H_6 w/ C_3H_6 (0.2 lb/hr), 8" level injection, test CP-188-1.
- - - ATR of C_6H_6 w/ C_3H_6 (0.4 lb/hr), 8" level injection, test CP-188-3.

while propylene itself disappears very slowly. The overall $(S/C)_{m,T}$ ratio at the 8 inch level was calculated to be 2.7, as shown in the bottom of Figure 9. This $(S/C)_{m,T}$ value appears to be high enough to steam reform any carbon formed from either propylene or benzene. However, the $(S/C)_{m,T}$ ratio at the 8 inch level was 2.2 for the case of 0.4 lb/hr propylene injection, which was carbon-forming. As discussed above, this $(S/C)_{m,T}$ value must be lower than the "critical" one for carbon-free operation at these conditions.

While this data does not produce information about the mechanism of carbon formation in the bed, it definitely shows that the steam reforming region of the bed is the most prone to carbon formation. In support of this is the above presented evidence that a reduced $(S/C)_m$ ratio at the ATR inlet, created here by olefin addition, has less effect on carbon formation than a similar $(S/C)_m$ reduction in the steam reforming part of the bed. Scanning electron microscope (SEM) examinations of catalyst samples used under carbon-forming conditions with pure benzene or n-tetradecane fuels also support this. As discussed in the previous section, surface carbon growths (mainly in the form of whiskers) were found on catalyst samples taken from the steam reforming region of the reformer, while no surface carbon was found on the NC-100 or the top ICI catalysts, where oxygen is present.

(C) ATR Of Mixtures Of Benzene And n-Tetradecane

Concluding the experimental studies of the autothermal reforming of sulfur-free hydrocarbon liquids, a series of tests with mixtures of paraffins and aromatics were run in the reformer. The purpose was to determine what effects aromatic and paraffinic hydrocarbon combinations have on catalyst bed temperatures, intermediate reaction products, and carbon formation, as compared to the pure component hydrocarbon data.

Mixtures of benzene and n-tetradecane were used because of the previous tests on them, individually, and the ease of following the hydrocarbon intermediates. Two mixtures were prepared in which the molar ratio of n-tetradecane to benzene, $(T/B)_m$, was set equal to 2.0 and 0.5, respectively. Tests were run at similar operating conditions as earlier tests with each of the component fuels. Fresh catalysts were loaded in the reformer prior to the first test of this series. In the middle catalyst zone, the ICI 46-1 catalyst was used to better control carbon formation. Tests CP-212 through 216 were run with the $(T/B)_m = 2.0$ mixture, while in tests CP-217 through 221, the $(T/B)_m = 0.5$ mixture was used. Table IV shows the operating conditions and summarizes the results from these tests. Corresponding axial bed temperatures are shown in Table IV-a.

Carbon-forming conditions for each mixture tested were determined and compared to those for the pure component hydrocarbons. These are depicted in Figure 10, in which the carbon formation lines determined for the mixtures are plotted along with carbon lines for neat benzene and n-tetradecane (see Figures 2 and 3). Similar inlet conditions, and the same catalyst types were used with all

TABLE IV
AUTOTHERMAL REFORMING OF MIXTURES
OF BENZENE AND N-TETRADECANE

TEST Q -	FUEL	(O ₂ /C) _m	(S/C) _m	(1) T _p °F	(2) MAX. BED TEMPERATURE		(3) m _f LB/HR	(4) S.V. HR ⁻¹	C A R B O N	(5) GAS PROBE AT INCHES	DRY GAS COMPOSITION, MOL %																																																																																																																																																																																																																																																																																																																																																																																																																																																																																																																																																																																																																																																																																																																																																																																																																																																																																																																																																																																																																																																																																																																																																																																																																																																																																																																																																																																																																																																																	
					T _{MAX} °F	AT IN.					H ₂	CO ₂	CO	HC _T	CH ₄	C ₂ H ₄	C ₂ H ₆	C ₃ H ₈	C ₃ H ₆	C ₄	C ₅	C ₆	C ₆ H ₆																																																																																																																																																																																																																																																																																																																																																																																																																																																																																																																																																																																																																																																																																																																																																																																																																																																																																																																																																																																																																																																																																																																																																																																																																																																																																																																																																																																																																																																					

TABLE IV (Cont'd)

TEST	FUEL	(O ₂ /C) _m	(S/C) _m	(1) T _p		(2) MAX. BED. TEMPERATURE		(3) m _f LB/HR	(4) S.V. HR ⁻¹	C A R B O N	(5) GAS PROBE AT INCHES	DRY GAS COMPOSITION, MOL %													
				°F	T _{MAX} °F	MAX IN.	AT																		
				H ₂	CO ₂	CO	HC _T	CH ₄	C ₂ H ₄	C ₂ H ₆	C ₃ H ₆	C ₃ H ₈	C ₄	C ₅	C ₆	C ₆ H ₆									
216	(T/B) _m = 2.0	0.29	1.5	1159	1525	6.0	5.5	9378	NO	INLET	0.06	0.37	0.54	2.36*	0.72	0.02	-	0.01	-	0.01	0.01	0.01	0.01	1.58	
				1148	1531	6.0	"	"	"	4	8.50	4.63	10.13	4.97*	0.63	1.69	0.13	0.54	-	0.36	0.21	0.21	0.21	1.20	
				1156	1531	6.0	"	"	"	6	30.63	9.09	15.71	4.00*	0.95	1.46	0.18	0.51	-	0.25	0.09	0.07	0.49		
				1142	1528	6.0	"	"	"	8	35.05	9.38	16.24	3.01	0.95	0.97	0.16	0.36	-	0.15	0.05	0.04	0.33		
				1153	1523	6.0	"	"	"	10	39.34	9.24	17.60	2.00	0.83	0.50	0.14	0.21	-	0.07	0.03	0.02	0.20		
				1161	1528	6.0	"	"	"	12	40.54	9.26	18.13	1.61	0.77	0.34	0.12	0.15	-	0.04	0.02	0.02	0.15		
217	(T/B) _m = 0.5	0.38	0.6	1158	1537	6.0	"	"	"	EXIT	41.12	9.81	17.51	1.29	0.74	0.20	0.11	0.09	-	0.03	0.01	0.01	0.10		
				1151	2011	5.8	6.5	9553	NO	4	23.90	4.34	22.78	2.93*	1.49	0.83	0.05	0.03	0.01	0.02	0.02	-	0.48		
				1150	2017	5.8	"	"	"	6	29.22	3.76	24.43	1.46*	1.03	0.22	0.02	0.01	-	-	-	-	0.18		
				1152	2014	5.8	"	"	"	8	30.38	3.59	24.84	1.01	0.83	0.08	0.01	-	-	-	-	-	0.09		
				1152	2010	5.8	"	"	"	10	31.72	3.42	24.97	0.73	0.65	0.03	0.01	-	-	-	-	-	0.04		
				1146	2005	5.8	"	"	"	EXIT	32.20	3.12	25.12	0.25	0.25	-	-	-	-	-	-	-	-		
218	(T/B) _m = 0.5	0.29	1.2	1148	1558	6.0	6.0	9520	YES	4	14.40	8.00	14.10	6.28*	0.78	1.97	0.16	0.61	0.01	0.37	0.14	0.11	2.13		
				1152	1571	6.0	"	"	"	6	33.49	9.11	18.67	2.55*	0.66	0.69	0.11	0.24	-	0.09	0.03	0.02	0.71		
				1152	1560	6.0	"	"	"	8	38.21	8.84	20.13	1.77	0.66	0.32	0.10	0.14	-	0.04	0.01	0.01	0.44		
				1150	1557	6.0	"	"	"	10	39.82	8.62	21.13	1.23	0.60	0.17	0.09	0.08	-	0.02	0.01	0.01	0.24		
				1153	1555	6.0	"	"	"	EXIT	39.95	8.74	19.97	1.04	0.58	0.11	0.07	0.05	-	0.02	0.01	0.01	0.18		
				1148	1854	5.8	6.5	9554	NO	4	20.80	5.15	21.44	3.95*	1.20	1.40	0.13	0.18	0.02	0.07	0.02	-	0.93		
219	(T/B) _m = 0.5	0.36	0.7	1146	1874	5.8	"	"	"	6	29.61	4.87	23.66	1.93*	1.12	0.39	0.05	0.02	-	0.01	0.01	-	0.33		
				1144	1870	5.8	"	"	"	8	32.62	4.22	24.42	1.04	0.77	0.11	0.03	0.01	-	-	-	-	0.12		
				1150	1872	5.8	"	"	"	10	33.23	4.35	24.37	0.83	0.71	0.04	0.02	-	-	-	-	-	0.06		
				1150	1851	5.8	"	"	"	EXIT	33.59	4.06	27.70	0.45	0.39	0.02	0.01	-	-	-	-	-	0.03		
				1150	1851	5.8	"	"	"	EXIT	33.59	4.06	27.70	0.45	0.39	0.02	0.01	-	-	-	-	-	0.03		
				1150	1851	5.8	"	"	"	EXIT	33.59	4.06	27.70	0.45	0.39	0.02	0.01	-	-	-	-	-	0.03		

TABLE IV (Cont'd)

TEST	FUEL	(O ₂ /C) _m	(S/C) _m	(1) T _p		(2) MAX. BED TEMPERATURE		(3) m _f	(4) S.V.	C	(5) GAS PROBE	DRY GAS COMPOSITION, MOL %																		
				°F	°C	T _{MAX} °F	TEMPERATURE					LB/HR	HR ⁻¹	A	R	B	O	N	H ₂	CO ₂	CO	HCl	CH ₄	C ₂ H ₄	C ₂ H ₆	C ₃ H ₈	C ₃ H ₆	C ₄	C ₅	C ₆
							AT	IN.	AT	INCHES																				
220	(T/B) _m = 0.5	0.40	0.6	1051		1953	6.5	6.25	9553	NO	4	15.15	5.65	19.13	4.56*	1.18	1.69	0.16	0.26	0.01	0.10	0.03	-	-	-	-	-	-	1.13	
				1046		1987	6.5	"	"	"	EXIT	31.48	3.42	24.55	0.31*	0.28	0.01	-	-	-	-	-	-	-	-	-	-	-	-	0.01
				1062		2007	6.0	6.25	9190	NO	4	23.44	3.93	23.19	2.76*	1.54	0.70	0.05	0.02	0.01	0.01	0.02	0.02	0.02	0.01	0.02	0.01	0.02	0.01	0.40
				1052		2001	6.0	"	"	"	6	27.84	3.40	24.56	1.76*	1.20	0.28	0.03	0.02	0.01	0.01	0.01	0.01	0.01	0.01	0.01	0.01	0.01	0.01	0.22
				1051		1998	6.0	"	"	"	8	29.77	3.11	25.09	1.03	0.83	0.08	0.02	-	-	-	-	-	-	-	-	-	-	-	0.10
				1057		1997	6.0	"	"	"	EXIT	30.69	2.83	25.16	0.34	0.29	0.01	-	-	-	-	-	-	-	-	-	-	-	-	0.03
221	(T/B) _m = 0.5	0.34	0.6	1145		1855	5.6	7.0	9473	YES	4	23.07	5.21	21.98	4.54*	1.47	1.59	0.14	0.18	0.02	0.07	0.02	-	-	-	-	-	-	1.05	
				1151		1861	5.6	"	"	"	EXIT	34.86	3.82	25.20	0.83*	0.74	0.02	0.03	0.01	-	-	-	-	-	-	-	-	-	0.03	
				1150		1889	5.0	7.0	8654	YES	4	20.25	3.59	23.60	5.26*	1.79	2.01	0.10	0.10	0.03	0.05	0.03	0.03	0.03	0.01	0.01	0.01	0.01	1.15	
				1160		1885	5.0	"	"	"	6	29.18	2.25	25.61	2.85	1.32	0.86	0.10	0.10	0.01	0.03	0.03	0.01	0.01	0.01	0.01	0.01	0.01	0.01	0.62
				1149		1887	5.0	"	"	"	8	31.33	1.10	26.88	1.59	1.08	0.21	0.06	0.03	-	-	-	-	-	-	-	-	-	0.21	
				1148		1877	5.0	"	"	"	EXIT	32.60	1.94	26.66	1.12	0.94	0.06	0.03	0.01	-	-	-	-	-	-	-	-	-	0.08	

(1) - (5) See Table III
 * Gaseous hydrocarbons not including n-tetradecane

TABLE IV-a
AUTOTHERMAL REFORMING OF MIXTURES OF BENZENE AND N-TETRADECANE
Longitudinal Bed Temperatures

TEST CP -	$(O_2/C)_m$	$(S/C)_m$	(1) T_p	S.V. hr^{-1}	BED TEMPERATURE, °F At (in. from Reactor Inlet)														
					0.5	3	4	5	6	7	8	9	10	11	12	13	14	15	
212	0.38	0.6	1050	9941	1145	1350	1451	1690	1792	1802	1751	1697	1680	1682	1594	1536	1502	1467	
213	0.31	1.2	1150	9549	1200	1320	1418	1540	1602	1611	1571	1523	1493	1502	1425	1365	1331	1308	
214	0.38	0.4	1055	10183	1200	1450	1520	1809	1901	1879	1841	1820	1817	1792	1711	1675	1640	1612	
215	0.34	0.8	1055	9456	1120	1275	1400	1597	1629	1587	1541	1524	1530	1466	1396	1363	1328	1314	
216	0.29	1.5	1155	9378	1190	1250	1329	1491	1537	1515	1466	1442	1453	1421	1339	1276	1241	1214	
217	0.38	0.6	1150	9553	1275	1560	1635	1958	2015	1949	1868	1832	1819	1790	1734	1700	1676	1665	
218	0.29	1.2	1152	9520	1196	1250	1325	1488	1575	1533	1472	1456	1469	1461	1409	1351	1301	1275	
219	0.36	0.7	1150	9554	1255	1410	1460	1762	1848	1785	1699	1670	1668	1661	1629	1596	1562	1539	
220-1	0.40	0.6	1050	9553	1134	1350	1392	1770	1965	1915	1814	1779	1770	1771	1747	1709	1674	1650	
220-3	0.40	0.5	1055	9190	1175	1530	1680	1886	2003	1909	1798	1768	1748	1714	1681	1676	1659	1635	
221-1	0.34	0.6	1150	9473	1350	1540	1589	1828	1852	1741	1644	1576	1513	1469	1434	1401	1385	1380	
221-4	0.34	0.4	1150	8654	1375	1650	1703	1889	1812	1675	1587	1515	1466	1449	1413	1392	1383	1379	

(1) Preheat Temperature, T.C. No. 13 (Figure 1)

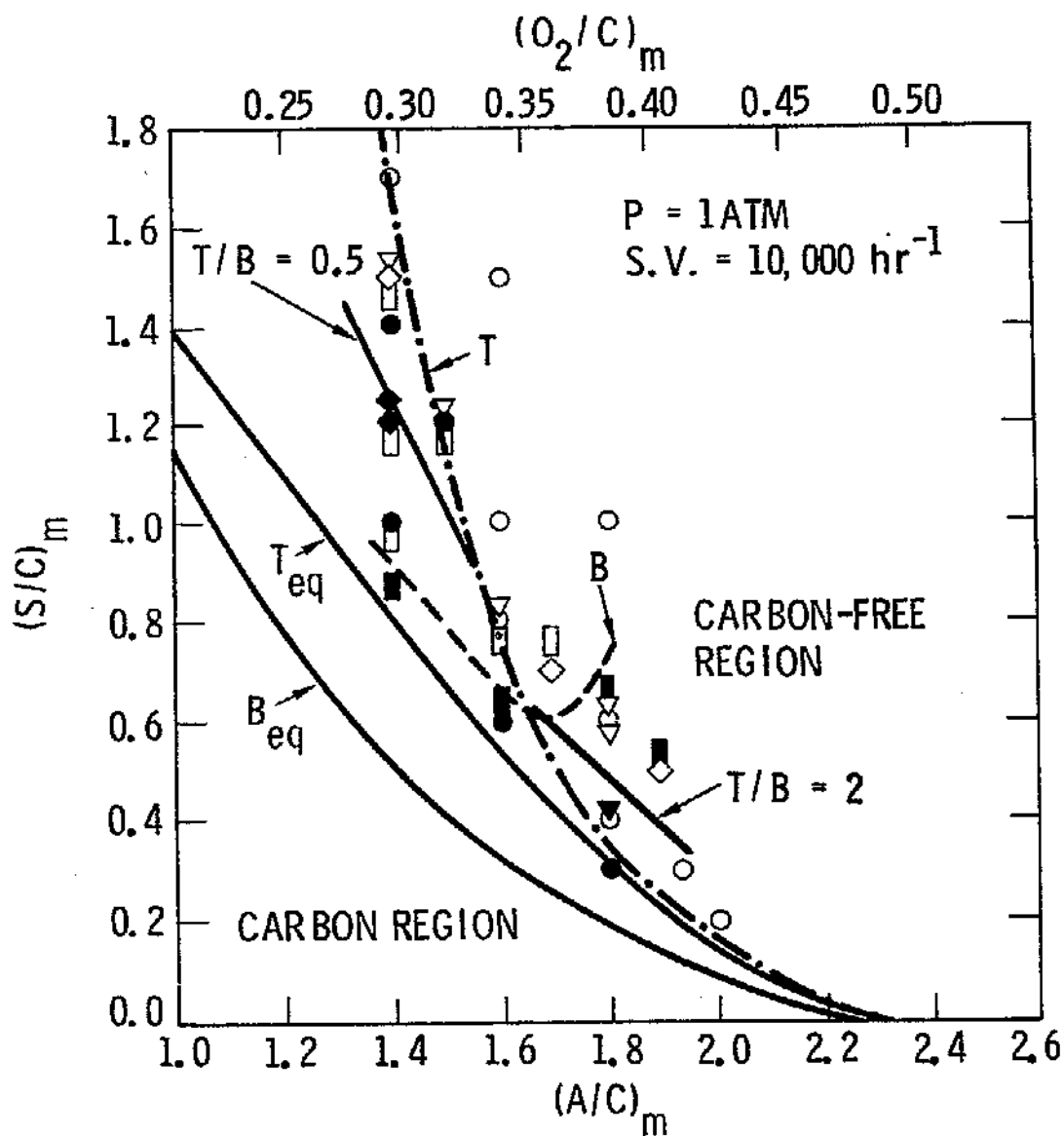


Figure 10. Autothermal Reforming of n-Tetradecane/Benzene Mixtures.
Carbon Formation Lines.
 ○ ●: n-Tetradecane ($C_{14}H_{30}$), neat
 ▼ ▽: Benzene solution ($C_{14}H_{30}/C_6H_6 = 2$, molar basis)
 ◇ ◆: Benzene solution ($C_{14}H_{30}/C_6H_6 = 0.5$, molar basis)
 □ ■: Benzene (C_6H_6), neat
 Open Symbols: Carbon-Free
 Closed Symbols: Carbon Formation

fuels with the exception of neat benzene, which had been tested with ICI 46-4 catalyst in the middle ATR zone.

The plots in Figure 10 clearly demonstrate that a synergistic effect exists in mixtures of benzene/n-tetradecane, whereby the carbon-formation line of the mixture lies between those of the component hydrocarbons. In the case of the mixture $(T/B)_m = 2.0$, the paraffinic character is prevailing; the carbon line diverges from equilibrium at low $(O_2/C)_m$ ratios, but not as much as the line for pure n-tetradecane. The reverse is true for the $(T/B)_m = 0.5$ mixture, which has more of the aromatic character. This line diverges from equilibrium at high $(O_2/C)_m$ ratios, but not as pronouncedly as the pure benzene line.

To further understand the causes of the observed synergism in benzene/n-tetradecane mixtures, reaction bed products and temperatures during ATR of mixtures were compared to these for the pure hydrocarbon components. Tables V and V-a show dry gas analyses and temperatures, respectively, from tests run at similar operating conditions with the mixtures and each pure hydrocarbon component. These data comparisons have revealed the following:

- (a) Bed temperatures for the mixtures were intermediate, i.e., they were lower than respective temperatures for neat benzene and higher than those for neat n-tetradecane.
- (b) The presence of benzene in the benzene/n-tetradecane mixtures appeared to limit the amount of intermediate hydrocarbons (primarily low molecular weight olefins) produced by cracking of n-tetradecane. As a result of

this, carbon formation was suppressed at low $(O_2/C)_m$ ratios where the deviation of the experimental from the theoretical carbon formation line was the largest for pure n-tetradecane (see Figure 2). The fact that the benzene/n-tetradecane mixtures had lower propensity for carbon formation than pure n-tetradecane at low $(O_2/C)_m$ ratios may be explained by the higher bed temperatures during ATR of the mixtures. The rate of carbon removal by steam reforming may exceed the rate of carbon formation (via paraffin cracking) at these temperatures, resulting in no carbon deposition in the bed.

- (c) The presence of n-tetradecane in the benzene/n-tetradecane mixtures appeared to control carbon formation from benzene at high $(O_2/C)_m$ ratios, where the deviation of the experimental from the theoretical carbon formation line was the largest for pure benzene (see Figure 3). This can be explained by the lower bed temperatures during ATR of the mixtures, which were caused by the endothermic cracking reactions of n-tetradecane. The rate of carbon formation via dehydrogenation of the benzene molecule would then be decreased because of lower temperatures. However, these temperatures are still high enough for steam reforming, so that the overall effect for paraffinic/aromatic mixtures in ATR is a carbon removal rate that is faster than in the case of the pure aromatic fuel at high $(O_2/C)_m$ ratios.

TABLE V

ATR COMPARISON OF BENZENE/N-TETRADECANE MIXTURES AND
THEIR PURE HYDROCARBON COMPONENTS

TEST #	FUEL	(O ₂ /C) _m	(S/C) _m	(1) T _p	(2) MAX. BED TEMPERATURE		(3) ṁ _f	(4) S.V.	C A R B O N	(5) GAS PROBE	DRY GAS COMPOSITION, MOL %														
					T _{MAX} °F	AT IN.					H ₂	CO ₂	CO	HCT	CH ₄	C ₂ H ₄	C ₂ H ₆	C ₃ H ₈	C ₃ H ₆	C ₄	C ₅	C ₆	C ₆ H ₆		
																								HR ⁻¹	AT INCHES
136	n-Tetradecane	0.38	0.6	1006	1742	5.0	7.19	10,000	NO	4	7.33	6.93	6.40	9.04*	1.62	4.57	0.26	1.31	0.01	0.78	0.29	-	-	0.20	
				1005	1744	5.0	"	"	"	6	28.11	6.21	17.11	4.43*	1.89	1.75	0.17	0.36	-	0.11	0.14	-	-	0.01	
				1005	1746	5.0	"	"	"	8	32.49	4.82	20.17	2.30	1.50	0.50	0.12	0.11	-	0.02	0.03	-	-	0.01	
				1017	1776	5.0	"	"	"	EXIT	35.40	4.48	21.13	1.08	0.87	0.03	0.06	0.01	-	-	0.04	-	-	0.01	
212	(T/B) _m = 2.0	0.38	0.6	1050	1798	6.3	7.0	9941	NO	4	8.50	5.63	13.50	8.16*	1.43	3.78	0.30	0.91	0.02	0.60	0.18	0.10	-	0.84	
				1052	1789	6.3	"	"	"	6	24.73	5.86	20.47	4.44*	1.72	1.88	0.18	0.21	0.02	0.06	0.01	-	-	0.36	
				1048	1777	6.3	"	"	"	B	32.73	4.30	23.52	1.70	1.02	0.42	0.09	0.06	-	0.01	-	-	-	0.10	
				1050	1805	6.3	"	"	"	EXIT	34.92	3.81	24.01	0.54	0.44	0.04	0.02	0.01	-	0.02	-	-	-	0.01	
217	(T/B) _m = 0.5	0.38	0.6	1151	2011	5.8	6.5	9553	NO	4	23.90	4.34	22.78	2.93*	1.49	0.83	0.05	0.03	0.01	0.02	0.02	-	-	0.48	
				1150	2017	5.8	"	"	"	6	29.22	3.76	24.43	1.46*	1.03	0.22	0.02	0.01	-	-	-	-	-	0.18	
				1152	2014	5.8	"	"	"	8	20.38	3.59	24.84	1.01	0.83	0.08	0.01	-	-	-	-	-	-	-	0.09
				1145	2005	5.8	"	"	"	EXIT	32.20	3.12	25.12	0.25	0.25	-	-	-	-	-	-	-	-	-	-
71-1	Benzene	0.38	0.6	1050	2010	4.8	7.0	10,000	YES	EXIT	27.82	3.18	27.12	0.03	0.02	-	-	-	-	-	-	-	-	0.01	

TABLE V (Cont'd)

TEST CP -	FUEL	(O ₂ /C) _m	(S/C) _m	(1) T _p	(2) MAX. BED TEMPERATURE		(3) m ² /HR	(4) S.V.	C	(5) GAS PROBE	DRY GAS COMPOSITION, MOL %												
					T _{MAX} °F	AT IN.					H ₂	CO ₂	CO	HCT	CH ₄	C ₂ H ₄	C ₂ H ₆	C ₃ H ₈	C ₃ H ₆	C ₄	C ₅	C ₆	C ₆ H ₆
					°F	IN.	HR ⁻¹	AT INCHES															
129	n-Tetradecane	0.34	0.8	1127	1664	5.7	6.43	8850	NO	4	12.50	6.55	13.10*	3.05	6.84	0.43	1.45	0.03	0.87	0.37	0.02	0.04	
				1132	1658	5.6	"	"	"	"	6	16.40	6.99	5.13*	2.26	1.74	0.22	0.45	0.03	0.19	0.06	0.11	0.06
				1135	1658	5.7	"	"	"	"	8	18.90	6.18	3.45	1.95	0.72	0.21	0.27	0.01	0.13	0.15	-	0.01
				1135	1663	5.6	"	"	"	"	EXIT	18.96	6.46	1.71	1.40	0.11	0.10	0.04	0.01	0.04	0.01	-	-
215	(T/B) = 2.0	0.34	0.8	1048	1631	5.9	6.5	9456	NO	4	14.50	8.25	5.90*	1.06	2.43	0.23	0.76	0.01	0.46	0.16	0.10	0.59	
				1055	1630	5.9	"	"	"	"	6	21.15	6.01	2.43*	0.95	0.73	0.15	0.25	-	0.09	0.02	0.02	0.22
				1045	1617	5.9	"	"	"	"	8	21.57	6.10	2.27	1.03	0.62	0.15	0.21	-	0.07	0.01	0.01	0.17
				1050	1613	5.9	"	"	"	"	10	22.45	5.52	1.56	0.91	0.28	0.13	0.11	-	0.03	0.01	-	0.09
203	Benzene	0.34	0.8	1052	1607	5.9	"	"	"	EXIT	22.19	5.90	1.11	0.83	0.09	0.09	0.05	-	0.01	-	-	0.04	
				1050	1811	6.0	6.0	9300	NO	4	7.58	2.80	7.49	0.09	0.24	-	0.01	0.02	0.06	0.07	0.01	6.99	
				1048	1807	6.0	"	"	"	"	6	22.93	6.62	1.01	0.08	0.02	-	-	0.01	0.02	-	0.88	
				1043	1813	6.0	"	"	"	"	EXIT	24.40	5.31	0.04	0.03	-	-	-	-	-	-	0.01	

(1) - (5) See Table III
 * Gaseous hydrocarbons not including n-tetradecane

TABLE V-a

COMPARISON OF ATR TEMPERATURES OBTAINED WITH BENZENE/N-TETRADECANE MIXTURES
AND THEIR PURE HYDROCARBON COMPONENTS

TEST CP ~	$(O_2/C)_m$	$(S/C)_m$	(1) T_p °F	S.V. hr^{-1}	BED TEMPERATURE, °F At (in. from Reactor Inlet)														
					0.5	3	4	5	6	7	8	9	10	11	12	13	14	15	
136	0.38	0.6	1020	10000	1180	1420	1600	1746	1678	1608	1553	1519	1476	1438	1421	1404	1390	1376	
212	0.38	0.6	1050	9940	1145	1350	1451	1690	1792	1802	1751	1697	1680	1682	1594	1536	1502	1467	
217	0.38	0.6	1150	9553	1275	1560	1635	1958	2015	1949	1868	1832	1819	1790	1734	1700	1676	1665	
71	0.38	0.6	1033	11000	1200	1875	1900	1986	1925	1968	1825	1716	1743	1719	1718	1723	1723	1713	
129	0.34	0.8	1130	8950	1155	1400	1511	1634	1657	1599	1545	1489	1458	1407	1365	1334	1304	1275	
215	0.34	0.8	1055	9456	1120	1275	1400	1597	1629	1587	1541	1524	1530	1466	1396	1363	1328	1314	
203	0.34	0.8	1054	9269	1041	1343	1310	1661	1813	1774	1730	1667	1615	1570	1528	1516	1509	1498	

(1) Preheat Temperature, T.C. No. 13 (Figure 1)

(D) ATR Of Sulfur-Containing Paraffins And Aromatics

In an effort to delineate the previously observed (6) conversion characteristics and carbon-forming limitations of No. 2 fuel oil in ATR, experimental work up to this point has focused on identifying the behavior of individual fuel components in the autothermal reformer. Differences in the ATR reactivity of sulfur-free paraffins and aromatics have been found, and the effects of the operating parameters on reaction intermediates, bed temperatures, and carbon formation have been determined.

An overall picture of the carbon formation lines for the various sulfur-free hydrocarbons used under similar conditions in the autothermal reformer is shown in Figure 11. The effects of chemical character, and molecular weight (or boiling point) on carbon formation in ATR can be seen from this figure. Experimental data from the ATR of No. 2 fuel oil (6) are also shown in Figure 11. This data cannot be used for a quantitative comparison of the fuel oil and pure hydrocarbon requirements for carbon-free operation (since a different catalyst (6) had been used in the low preheat ($\sim 1150^{\circ}\text{F}$) tests with No. 2 fuel oil). However, from a qualitative comparison of the shape and location of these curves, it appears that the chemical character (e.g., aromatic content) and the boiling point effects are not enough to explain the extremely pronounced propensity of fuel oil for carbon formation in ATR.

The No. 2 fuel oil used in the earlier JPL work (6) consisted of a mixture of paraffins (71% vol.), aromatics (22% vol.), and olefins (7% vol.). The sulfur content of that oil was 0.35% wt. As discussed in the previous section, mixtures of paraffins and aromatics exhibit a synergism with respect to carbon

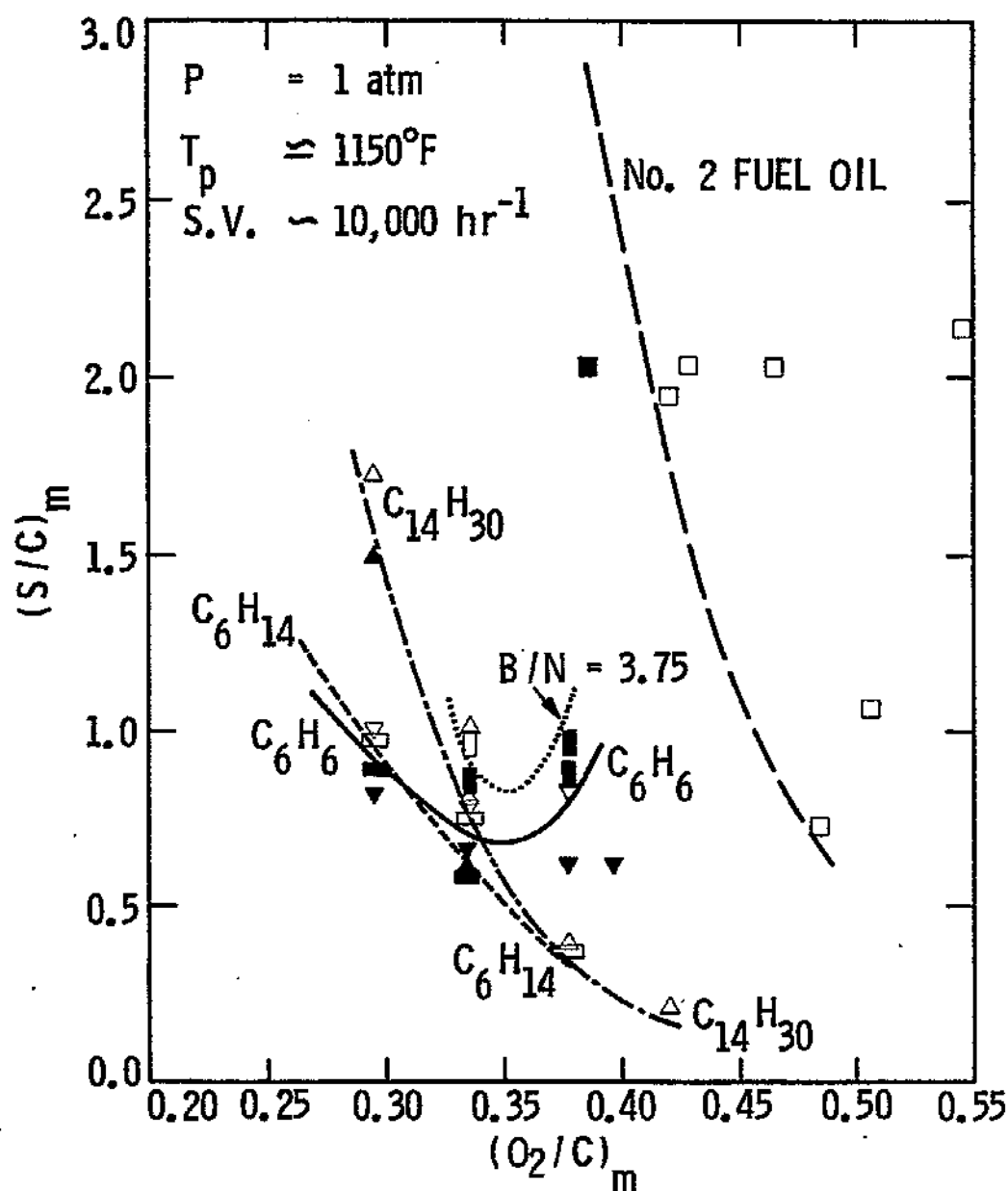


Figure 11. ATR of Various Hydrocarbon Liquids.
 Experimental Carbon Formation Lines.
 □ ■ : No. 2 Fuel Oil, Catalyst Configuration A (Ref. 6).
 ▽ ▼ : Benzene (C_6H_6)
 □ ■ : Benzene/Naphthalene, $(B/N)_m = 3.75$ } Catalyst
 □ ■ : n-Hexane (C_6H_{14}) } Configuration B (Fig. 1)
 △ ▲ : n-Tetradecane ($C_{14}H_{30}$)
 Open Symbols: Carbon-Free
 Closed Symbols: Carbon Formation

formation in ATR. Hence, the steam requirements for carbon-free operation with No. 2 fuel oil should be lower than those corresponding to its heaviest aromatic components (at high O_2/C ratios) or its heaviest paraffinic components (at low O_2/C ratios). Obviously, what remains unanswered at this point is the relative importance of the sulfur content of fuels with respect to carbon formation in ATR. In the following, results from preliminary tests with thiophene-contaminated n-tetradecane and benzene are presented. This work was undertaken in order to study the conversion and degradation effects of fuel sulfur on the catalyst. It has been found that No. 2 fuel oil can contain up to 90% thiophenic sulfur compounds (15). Thus, thiophene is a good model sulfur compound for heavy distillate fuels.

ATR of Thiophene-containing n-Tetradecane

The effect of sulfur in the ATR characteristics of paraffins was examined first by using n-tetradecane contaminated with thiophene, 2000 ppmw (by weight). This amount of thiophene is equivalent to 762 ppmw sulfur. Tests with this mixture were run at similar conditions as earlier ones for n-tetradecane alone. These tests were performed to determine what effect the conversion of sulfur compounds would have on the autothermal reformer temperatures, catalyst activity, intermediate reaction products, and carbon-forming tendency.

Table VI summarizes the experimental data collected from tests with the n-tetradecane/thiophene mixture at three sets of operating conditions, which were carbon-free for pure n-tetradecane (11). A fresh catalyst bed was loaded in the reactor prior to test CP-222, and again prior to test CP-229. As in tests with neat n-tetradecane, the ICI catalyst used in the second catalyst zone was of the 46-1 type, which contains potassium oxide as a soot-suppres-

TABLE VI

ATR PERFORMANCE COMPARISON OF THIOPHENE-CONTAINING
N-TETRADECANE AND PURE N-TETRADECANE

TEST OP -	FUEL	(O ₂ /C) _m	(S/C) _m	(1) T _p	(2) MAX. BED TEMPERATURE		(3) m ³ /HR	(4) S.V. HR ⁻¹	C A R B O N	(5) GAS PROBE	DRY GAS COMPOSITION, MOL %													
					T _{MAX} °F	AT IN.					CO ₂	CO	HCT	CH ₄	C ₂ H ₄	C ₂ H ₆	C ₃ H ₆	C ₃ H ₈	C ₄	C ₅	C ₆	C ₆ H ₆		
					°F	INCHES	H ₂																	
160	n-Tetradecane	0.36	0.6	1038	1719	5.3	7.50	10000	NO	INLET		0.24	0.56	0.48	43.72	4.28	21.13	0.51	17.16	0.14	0.15	0.15	0.16	0.04
	"	"	"	1037	1707	"	"	"	"	4		7.87	8.52	11.59	10.01	2.00	4.75	0.32	1.31	0.02	0.98	0.37	0.26	0.09
	"	"	"	1040	1713	"	"	"	"	6		28.08	5.09	17.82	5.30	2.00	2.17	0.23	0.55	0.01	0.22	0.06	0.06	0.05
	"	"	"	1034	1725	"	"	"	"	EXIT		35.57	4.74	20.80	1.71	1.27	0.21	0.12	0.07	-	0.02	-	0.20	0.01
234	n-Tetradecane			1102	2007	7.0	7.20	9208	NO	4		4.50	3.70	12.50	20.83	3.95	13.40	0.23	1.59	0.13	1.01	0.20	0.13	0.13
	w/Thiophene	0.38	0.4	1131	2002	"	"	"	"	6		20.25	3.40	21.00	10.95	4.89	5.66	-	0.13	0.05	0.08	0.01	-	0.13
	"	"	"	1124	1990	"	"	"	"	8		26.30	3.58	22.03	7.84	4.11	3.46	0.09	0.04	0.01	0.04	-	-	0.09
	"	"	"	1130	2030	6.7	7.20	9208	NO	4		6.02	4.85	14.50	18.44	4.75	11.66	0.15	0.96	0.13	0.55	0.08	-	0.16
235	"	"	"	1141	2025	"	"	"	"	6		22.78	4.11	20.97	9.24	4.53	4.43	-	0.06	0.04	0.06	0.01	-	0.11
	"	"	"	1134	2027	"	"	"	"	8		27.34	3.66	22.34	7.16	3.86	2.56	0.60	0.01	0.01	0.03	0.01	-	0.08
	"	"	"	1099	1970	"	"	"	"	EXIT		31.56	2.47	24.14	2.20									
	"	"	"																					
146	n-Tetradecane	0.38	0.3	1055	1892	4.7	8.2	10000	YES	4		9.60	5.65	11.63	14.00	4.09	7.92	0.49	1.20	0.05	0.02	0.11	0.02	0.09
	"	"	"	1051	1916	"	"	"	"	6		29.49	2.01	22.86	3.52	2.45	0.82	0.13	0.09	-	0.02	-	-	0.01
	"	"	"	1053	1922	"	"	"	"	8		31.96	1.17	24.33	2.30	1.97	0.20	0.09	0.03	-	-	-	-	0.01
	"	"	"	1055	1980	"	"	"	"	EXIT		32.76	0.99	25.20	1.65	1.55	0.03	0.06	0.01	-	-	-	-	-

TABLE VI (Cont'd)

TEST CP -	FUEL	(O ₂ /C) _m	(S/C) _m	(1) T _p	(2) MAX. BED TEMPERATURE		(3) m _f	(4) S.V. hr ⁻¹	C A R B O N	(5) GAS PROBE	DRY GAS COMPOSITION, MOL %														
					T _{MAX} °F	AT IN.					H ₂	CO ₂	CO	HC _T	CH ₄	C ₂ H ₄	C ₂ H ₆	C ₃ H ₆	C ₃ H ₈	C ₄	C ₅	C ₆	C ₆ H ₆		
																								AT INCHES	
222	n-Tetradecane w/Thiophene	0.38	0.6	1021	2000	8.0	7.20	10000	NO	EXIT	32.24	4.35	22.05	4.38	2.36	1.75	0.14	0.08	-	0.02	-	-	-	-	0.03
226	"	0.38	0.6	1011	1959	8.9	7.20	10000	NO	INLET	-	-	-	0.96	0.06	0.21	0.01	0.16	-	0.14	0.13	0.16	0.09		
224	"	0.38	0.6	1048	1985	8.5	7.20	10000	NO	4	0.22	2.45	2.19	4.70	0.58	2.03	0.09	0.64	-	0.34	0.32	0.44	0.26		
	"	"	"	1051	1970	"	"	"	"	6	0.27	2.76	7.13	18.55	2.70	9.75	0.21	2.39	0.04	1.83	0.63	0.68	0.32		
	"	"	"	1037	1968	"	"	"	"	8	1.49	4.49	19.75	13.73	5.00	7.78	0.06	0.35	0.11	0.20	0.04	0.17	0.02		
225	"	0.38	0.6	1048	1995	9.0	7.20	10000	NO	10	23.97	4.54	20.98	10.10	4.70	4.97	0.04	0.15	0.03	0.09	0.01	0.11	-		
226	"	"	"	1060	1989	8.9	7.20	10000	NO	12	28.89	4.51	21.31	4.25	3.10	1.09	0.02	-	-	-	-	0.04	-		
	"	"	"	1078	1963	"	"	"	"	14	29.97	4.63	21.64	4.34	3.12	1.16	0.02	-	-	-	-	0.04	-		
	"	"	"	1078	1957	"	"	"	"	EXIT	31.89	4.11	22.86	3.62	2.86	0.65	0.07	0.01	-	-	-	0.03	-		
136	n-Tetradecane	0.38	0.6	1006	1762	5.0	7.19	10000	NO	4	7.33	6.93	6.40	9.04	1.62	4.57	0.26	1.31	0.01	0.78	0.29	-	0.20		
	"	"	"	1005	1744	"	"	"	"	6	28.11	6.21	17.11	4.43	1.89	1.75	0.17	0.36	-	0.11	0.14	-	0.01		
	"	"	"	1005	1746	"	"	"	"	8	32.49	4.82	20.17	2.30	1.50	0.50	0.12	0.11	-	0.02	0.03	-	0.01		
	"	"	"	1017	1776	"	"	"	"	EXIT	35.40	4.48	21.13	1.08	0.87	0.30	0.06	0.01	0.01	-	0.04	-	0.01		
233	n-Tetradecane w/Thiophene	0.36	0.6	1111	1910	8.8	7.52	10000	NO	4	0.05	2.02	3.13	10.18	1.21	5.00	0.27	1.40	0.18	1.02	0.50	0.53	0.07		
	"	"	"	1114	1915	"	"	"	"	6	0.72	5.01	14.50	20.45	4.53	13.45	0.27	1.26	0.11	0.63	0.03	0.01	0.19		
	"	"	"	1109	1904	"	"	"	"	8	1.54	4.00	17.50	8.28	3.31	4.45	0.18	0.16	-	0.07	-	0.01	0.10		
231	n-Tetradecane w/Thiophene	0.36	0.6	1118	1964	8.5	7.52	10000	NO	10	27.10	4.39	21.68	-	-	-	-	-	-	-	-	-	-		
	"	"	"	1119	1961	"	"	"	"	12	30.80	4.59	21.88	-	-	-	-	-	-	-	-	-	-		
	"	"	"	1116	1949	"	"	"	"	14	31.72	4.57	21.89	-	-	-	-	-	-	-	-	-	-		
229	"	0.36	0.6	1057	1964	8.0	7.52	10000	NO	EXIT	33.57	4.41	22.64	4.83	3.29	1.27	0.15	0.06	-	0.01	-	0.05	-		

(1) - (5) See Table III
 * Gaseous hydrocarbons not including n-tetradecane

sant. Data from tests with neat n-tetradecane run earlier (11) at the same conditions are also shown in Table VI for comparison. The following observations were made during this series of autothermal reforming tests:

- (a) Temperatures with the mixture of n-tetradecane and thiophene were lower in the upper half of the bed and higher in the lower half of the bed than respective temperatures with neat n-tetradecane. The peak temperature with the mixture was recorded at least 3 inches below that for n-tetradecane, indicating that the activity of the front-end catalyst was lower in the presence of sulfur. The value of the maximum temperature was higher by about 200°F in the case of the mixture, probably because fresh catalyst was used in both tests. Figure 12 shows axial bed temperature profiles for n-tetradecane, neat and with thiophene at $(O_2/C)_m = 0.36$, $(S/C)_m = 0.60$. The profile for the mixture corresponds to test CP-223 in which the maximum temperature was recorded at 9 inches below the reactor inlet. However, the initial location of the temperature peak for these conditions was at 8 inches from the inlet (test CP-229) indicating that the catalyst in the oxidation zone was rapidly being poisoned during exposure to the sulfur-containing fuel.
- (b) While no carbon formation was detected with the n-tetradecane/thiophene mixtures at the conditions of Table VI, the amounts of intermediate reaction products formed via cracking reactions were higher with the mixtures than with n-tetradecane. This was true throughout the length of the bed except at the front 4 to 5 inches from the bed inlet. Figure 13 depicts axial composition profiles corresponding to the temperature profiles of

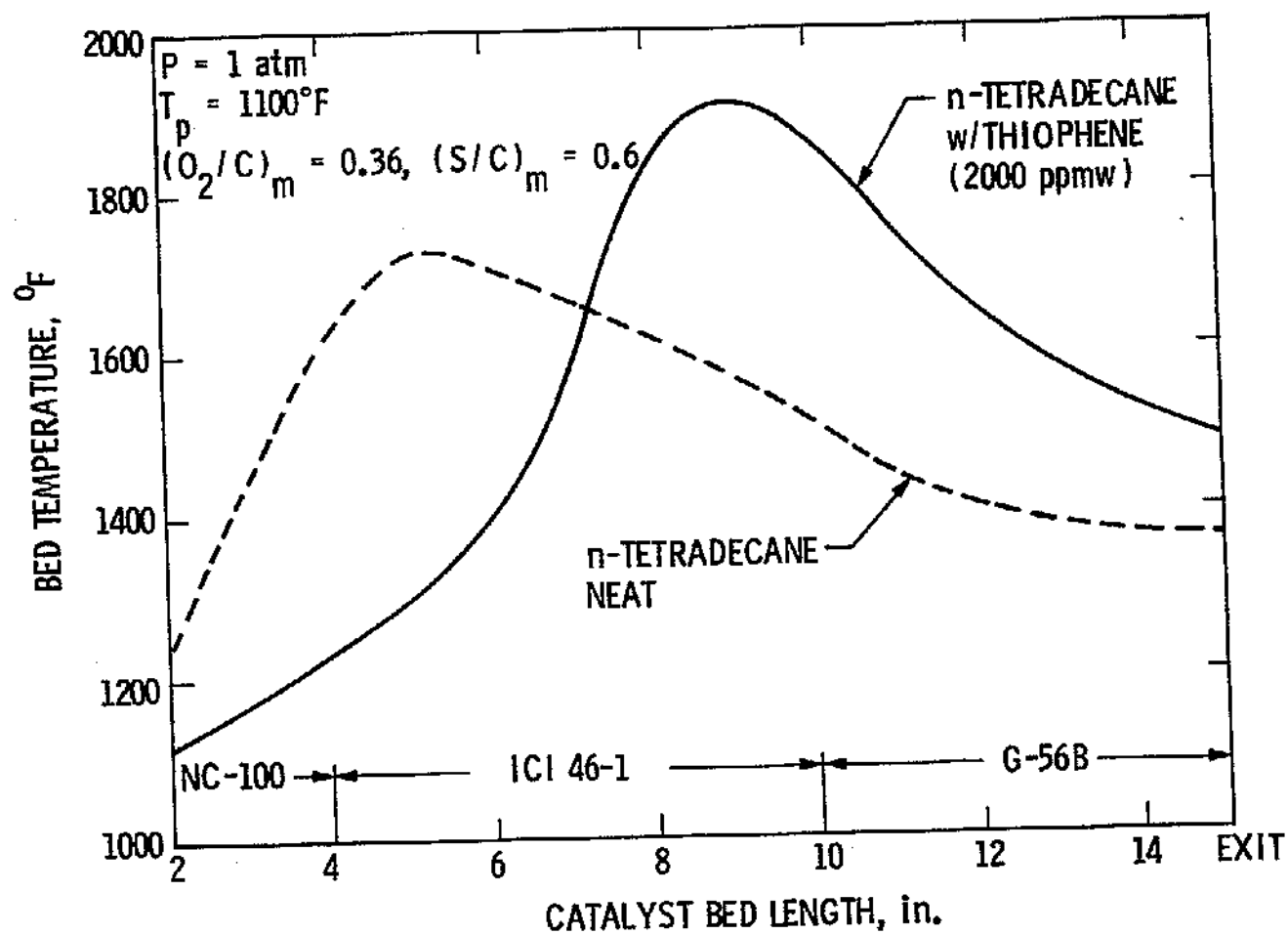


Figure 12. Autothermal Reforming of n-Tetradecane, neat with 2000 ppmw Thiophene. Axial Bed Temperature Profiles.

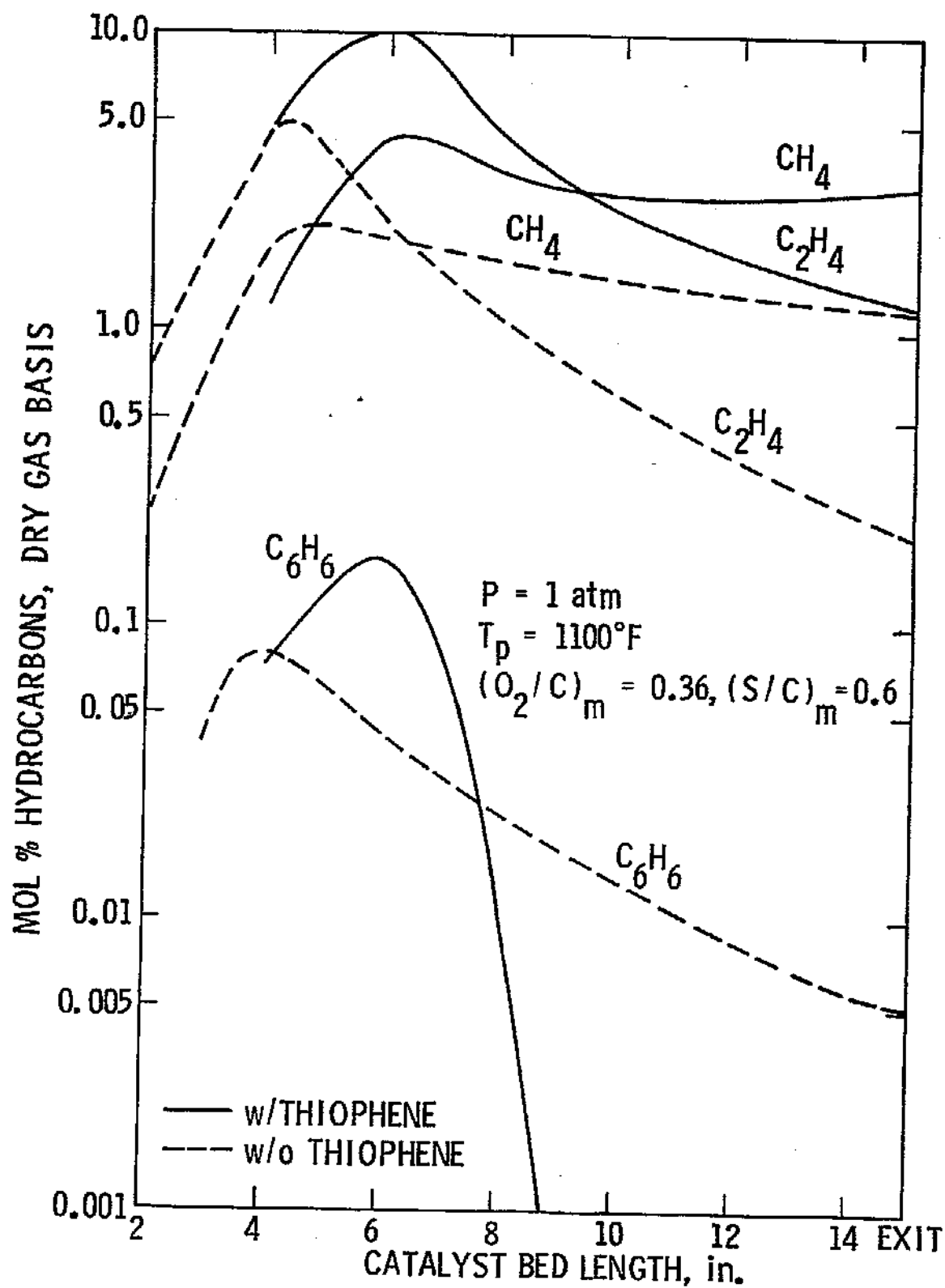


Figure 13. Autothermal Reforming of n-Tetradecane, neat
 and with 2000 ppmw Thiophene.
 Axial Bed Composition Profiles.

Figure 12. In both cases, i.e., n-tetradecane and the n-tetradecane/thiophene mixture, the intermediate hydrocarbons peaked just upstream of the respective temperature peak. However, the concentrations of ethylene, methane, benzene etc., were much higher for the mixture. In addition, the methane conversion in the steam reforming region of the bed was limited, and a higher methane leakage was measured at the bed exit when the mixture was used in ATR.

- (c) Along with hydrocarbon analysis, gas samples from different levels of the catalyst bed were analyzed for sulfur compounds by G.C. (FPD). In the partial oxidation region of the bed, unconverted thiophene was the only sulfur-containing species found in the gas phase. However, the amount of thiophene detected in this region was lower than at the reactor inlet, indicating that sulfur had reacted with the catalyst/support and formed a stable compound on the solid surface. Around the location of the temperature peak, and further down the bed (in the steam reforming region), a higher rate of thiophene conversion was observed, and other sulfur products, namely H_2S , COS and traces of CS_2 , appeared in the gas phase. Figure 14 shows axial profiles of H_2S , COS and thiophene in the bed. Since all sulfur species were not quantitatively analyzed, Figure 14 is intended as a qualitative plot only. Thus, an arbitrary logarithmic scale is used on the ordinate of Figure 14. The H_2S profile was found to be almost flat throughout the G-56B catalyst zone, and about two orders of magnitude higher than the COS, which peaked at the position of the temperature peak, gradually decreasing thereafter.

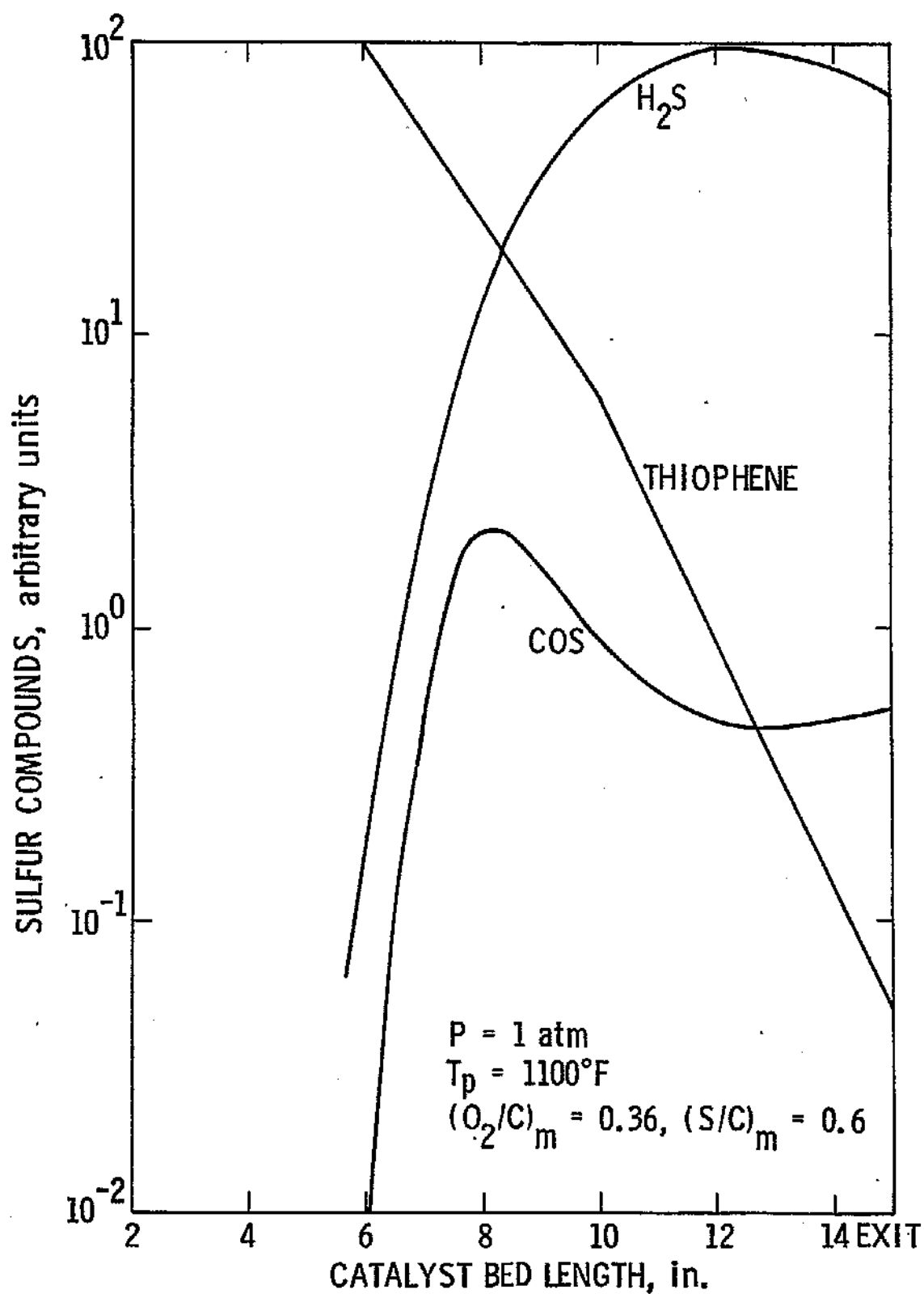


Figure 14. Autothermal Reforming of n-Tetradecane with 2000 ppmw Thiophene. Gas Phase Axial Profiles of Sulfur Compounds.

- (d) Catalyst samples from different bed locations were examined by SEM/EDAX. No surface carbon was detected in any of these samples. However, sulfur was found (by EDAX) on the surface of all three types of catalysts (NC-100, ICI 46-1, G-56B) throughout the bed. Figure 15 shows a SEM photomicrograph of the surface of ICI 46-1 catalyst taken from a location upstream of the maximum temperature region of the bed. A large part of this surface is comprised of a crystalline material, perhaps inorganic sulfate. Quantitative sulfur analysis was not made here since the total run times of these catalysts with the sulfur-containing fuel were not sufficiently long to make such an analysis conclusive at this point.

The above exploratory investigation of the effects of fuel sulfur in the ATR of paraffins has indicated the following:

- (i) At the front end of the bed where partial oxidation of the fuel takes place, thiophene reacts with the catalyst/support surface and, presumably, forms some stable surface compound. Gases from this part of the bed contain no COS, indicating that any COS produced there is retained by the solid or rapidly reacted. During this process, catalyst sites active for the oxidation reaction of the hydrocarbon fuel are being depleted, temperatures are lower, and the location of the temperature maximum is shifted down the bed, indicating catalyst deactivation. It is interesting to note that it took less than 1 hour of run time for temperature profiles such as in Figure 12 to develop, indicating a more rapid loss in activity than when no sulfur is present in the fuel. However, temperatures in this part of the bed appear to be high enough for exten-



Figure 15. SEM photomicrograph of the surface of ICI 46-1 catalyst used in ATR of the n-tetradecane/thiophene mixture at $P = 1$ atm, $T_p = 1150^\circ\text{F}$, $(\text{O}_2/\text{C})_m = 0.38$, $(\text{S}/\text{C})_m = 0.6$, and $\text{S.V.} = 10,000 \text{ hr}^{-1}$.

sive steam cracking (in the gas phase) and thermocracking of the fuel on the catalyst/support surface (or in the gas phase) to take place, as was observed experimentally.

- (ii) In the vicinity of the temperature peak, carbonyl sulfide becomes measurable in the gas phase (see Figure 14), and peaks upstream of the temperature peak. In the same region, H_2S is rapidly increasing to a peak in parallel with more hydrogen produced from the main reactions. Further down the bed, a lower amount of COS is observed in the gas phase, probably because it hydrolyzes to H_2S and/or reacts with the catalyst surface.
- (iii) In the steam reforming region of the bed, in the absence of oxygen, the predominant sulfur species is H_2S . Temperatures in this region, though decreasing, are very high (see Figure 12), steam reforming can proceed at a fast rate, and there may be enough hydrogen available so that any potential surface sulfide of nickel becomes unstable (5). The flat H_2S profile in this part of the bed (see Figure 14) is indicative of no or very little H_2S /solid interaction. The sulfur laydown in the lower end of the catalyst bed identified by SEM/EDAX may be due to transients in the operating conditions. To prove this point, however, additional experiments under well controlled conditions are necessary.
- (iv) While no carbon formation took place in the autothermal reformer at the conditions of Table VI, one may predict (based on the amounts of intermediate hydrocarbons in the gases) that carbon would be

formed in the case of the mixture by decreasing slightly the $(S/C)_m$ ratio at the inlet, while leaving all other parameters the same (11). The new conditions would still be carbon-free for the pure hydrocarbon, hence the propensity for carbon formation appears to be higher for the sulfur-containing hydrocarbon.

ATR of Thiophene-containing Benzene

Following tests with sulfur-containing paraffins, autothermal reforming tests were performed with benzene in which 1750 ppmw thiophene (or 667 ppmw sulfur) had been added in order to examine the effect of sulfur on the ATR characteristics of aromatic fuels.

Tests CP-237 through 239 were run at $(O_2/C)_m = 0.34$, $(S/C)_m = 0.80$.

Fresh catalyst was loaded in the reactor prior to test CP-237. In the middle catalyst zone, the ICI 46-4 catalyst was used as in earlier tests with neat benzene (10). In tests CP-241 through 243, the same operating conditions were used on a fresh batch of the same catalyst types. Table VII summarizes the data collected from these tests, and also lists data from an earlier test, CP-203, run with benzene for comparison.

Sulfur conversion (and deposition) in the upper part of the catalyst bed affected bed temperatures in a similar way to the case of n-tetradecane/thiophene mixture. As shown in Figure 16, the axial temperature profile for benzene/thiophene was displaced by 4 inches down the bed from that corresponding to neat benzene. A higher peak temperature was observed with the mixture, probably due to its proximity with the G-56B catalyst which has a higher nickel loading than the ICI 46-4 catalyst. As with n-tetradecane, the sulfur poison-

TABLE VII

ATR PERFORMANCE COMPARISON OF THIOPHENE-CONTAINING BENZENE AND
PURE BENZENE

TEST OP -	FUEL	(O ₂ /C) _m	(S/C) _m	(1) T _P °F	(2) MAX. BED TEMPERATURE		(3) m _f LB/HR	(4) S.V. HR ⁻¹	C A R B O N	(5) GAS PROBE	DRY GAS COMPOSITION, MOL %																
					T _{MAX} °F	AT IN.					H ₂	CO ₂	CO	HC _T	CH ₄	C ₂ H ₄	C ₂ H ₆	C ₃ H ₆	C ₃ H ₈	C ₄	C ₅	C ₆	C ₆ H ₆				
239	Benzene	0.34	0.8	1079	2074	9.0	6.01	9440	YES	INLET	6	-	0.07	0.38	7.68	-	-	-	-	-	-	-	-	-	0.01	7.67	
238	w/Thiophene	"	"	1076	2049	9.8	"	"	"	"	8	10.07	5.82	21.30	7.09	0.49	0.62	0.01	0.04	0.12	0.14	-	-	-	-	-	5.67
239	"	"	"	1085	2046	"	"	"	"	"	10	22.40	5.28	24.28	3.42	0.29	0.08	0.04	0.01	0.02	0.04	-	-	-	-	-	2.94
	"	"	"	1079	2082	"	"	"	"	"	12	22.32	5.15	24.47	2.81	0.28	0.08	0.03	0.01	0.01	-	-	-	-	-	2.36	
	"	"	"	1072	2073	"	"	"	"	"	14	28.77	5.25	25.53	2.17	0.16	0.02	-	-	-	-	-	-	-	-	1.99	
	"	"	"	1073	2055	"	"	"	"	"	EXIT	28.46	5.37	25.64	1.66	0.14	0.02	-	-	-	-	-	-	-	-	1.50	
	"	"	"	1083	2055	"	"	"	"	"	EXIT	30.36	5.63	25.56	0.56	0.11	0.01	-	-	-	-	-	-	-	-	0.43	
241	Benzene	0.34	0.8	1086	2009	8.7	6.01	9440	YES	4	4	0.05	3.06	11.50	11.33	0.12	4.07	-	0.03	0.10	0.04	0.07	0.07	0.07	0.07	6.89	
	w/Thiophene	"	"	1069	2011	"	"	"	"	EXIT	30.66	30.66	5.39	25.60	0.37	0.10	-	-	-	-	-	-	-	-	-	0.27	
243	Benzene	0.34	0.8	1074	2074	9.8	6.01	9440	YES	EXIT	30.14	30.14	5.16	25.28	0.80	0.14	0.01	-	-	-	-	-	-	-	-	0.65	
203	Benzene	0.34	0.8	1050	1811	6.0	6.00	9300	NO	4	4	2.73	2.80	7.58	7.49	0.09	0.24	-	0.01	0.06	0.07	0.01	0.01	0.01	0.01	6.99	
	"	"	"	1048	1807	"	"	"	"	6	6	26.35	6.62	22.93	1.01	0.08	0.02	-	-	0.01	0.02	-	-	-	-	0.88	
	"	"	"	1043	1813	"	"	"	"	EXIT	30.05	30.05	5.31	24.40	0.04	0.03	-	-	-	-	-	-	-	-	-	0.01	
240	Benzene	0.29	1.0	1187	2043	9.8	7.01	11020	NO	6	6	-	7.80	1.25	7.87	0.03	0.01	0.01	-	-	-	-	-	-	-	7.82	
242	w/Thiophene	"	"	1053	2000	10.2	7.01	"	"	EXIT	31.23	31.23	7.32	23.93	1.19	0.07	0.01	-	-	-	-	-	-	-	-	1.11	
61	Benzene	0.29	1.0	1055	1700	5.8	7.00	11020	NO	EXIT	35.75	35.75	7.03	22.75	0.27	0.20	-	-	-	-	-	-	-	-	-	0.07	

(1) - (5) See Table III

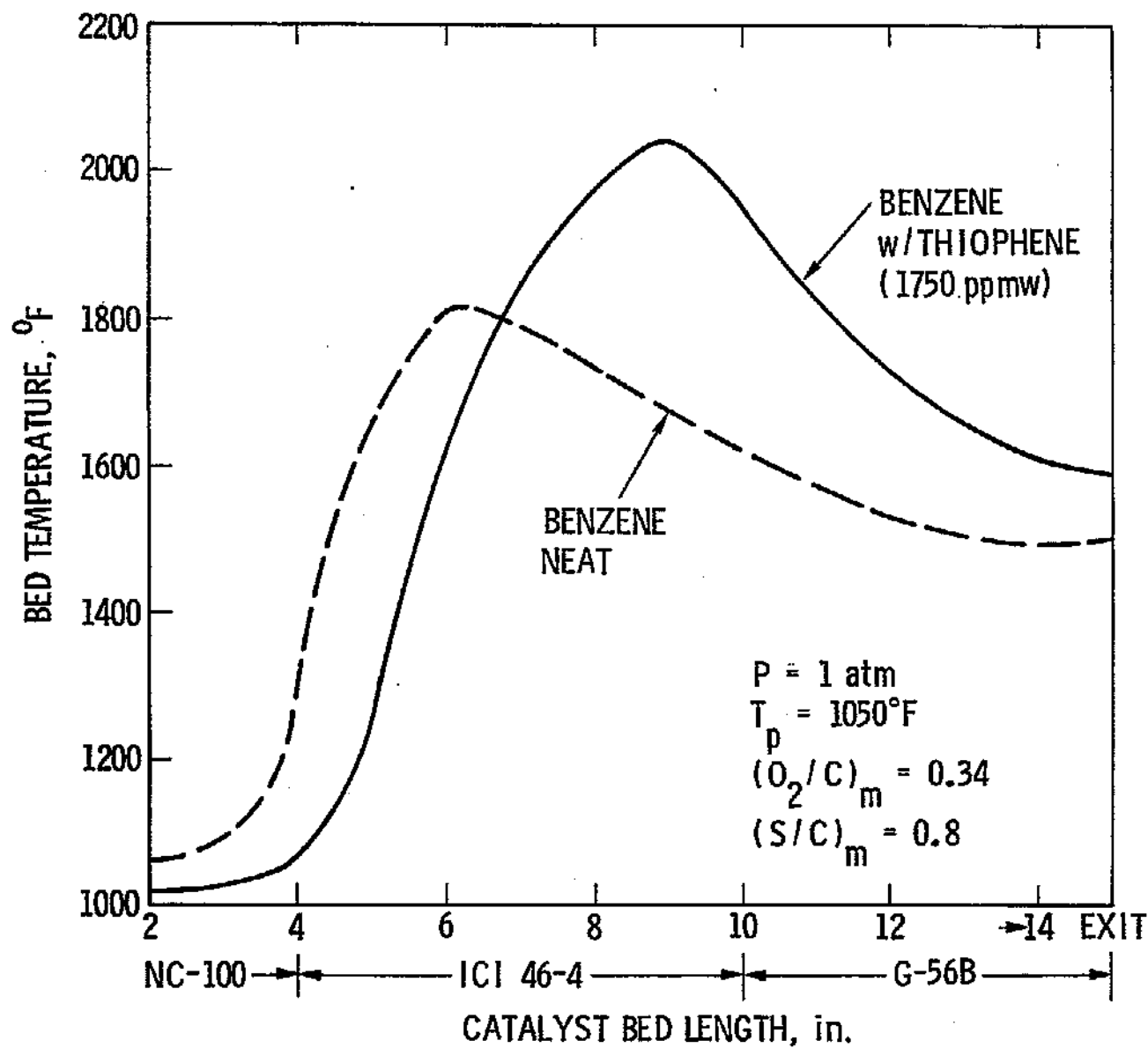


Figure 16. Autothermal Reforming of Benzene, neat and with 1750 ppmw Thiophene.
 Axial Bed Temperature Profiles.

ing of the front-end catalyst was rapid, pushing the temperature peak down the bed in later runs (Table VII).

Analysis of gas samples from various bed locations is given in Table VII, and axial profiles for CH_4 , C_2H_4 , C_3H_6 , and C_6H_6 are shown in Figure 17 for the conditions of Figure 16. Higher amounts of olefins and methane were produced throughout the catalyst bed, and more unconverted benzene was detected in the exhaust gases with the benzene/thiophene mixture than with benzene alone. Carbon was formed when the mixture was used at these conditions, which were carbon-free for neat benzene (test CP-203). Because of the higher amount of unconverted benzene and higher temperatures around the temperature peak region, the rate of carbon formation there might have been enhanced, perhaps via dehydrogenation of the benzene molecule.

Gas phase sulfur products, H_2S and COS , appeared early in the bed during the ATR of benzene/thiophene. Qualitative plots of the axial bed profiles of these two compounds are shown in Figure 18. A flat profile is observed for H_2S , while COS peaks close to the location of the temperature peak (similar to the plots of Figure 14). Thiophene could not be detected by the G.C. (FPD) in these tests because it was masked by benzene which had the same retention time as thiophene in the Poropak QS column of the G.C.

Another set of conditions with benzene/thiophene were tested in tests CP-240, 242 and 244, with $(\text{O}_2/\text{C})_{\text{m}} = 0.29$, $(\text{S}/\text{C})_{\text{m}} = 1.0$ (Table VII). By comparing this data to test CP-61 (neat benzene) similar reactivity can be seen concerning the effect of sulfur on conversion efficiency and propensity for carbon formation in the ATR of aromatic hydrocarbons.

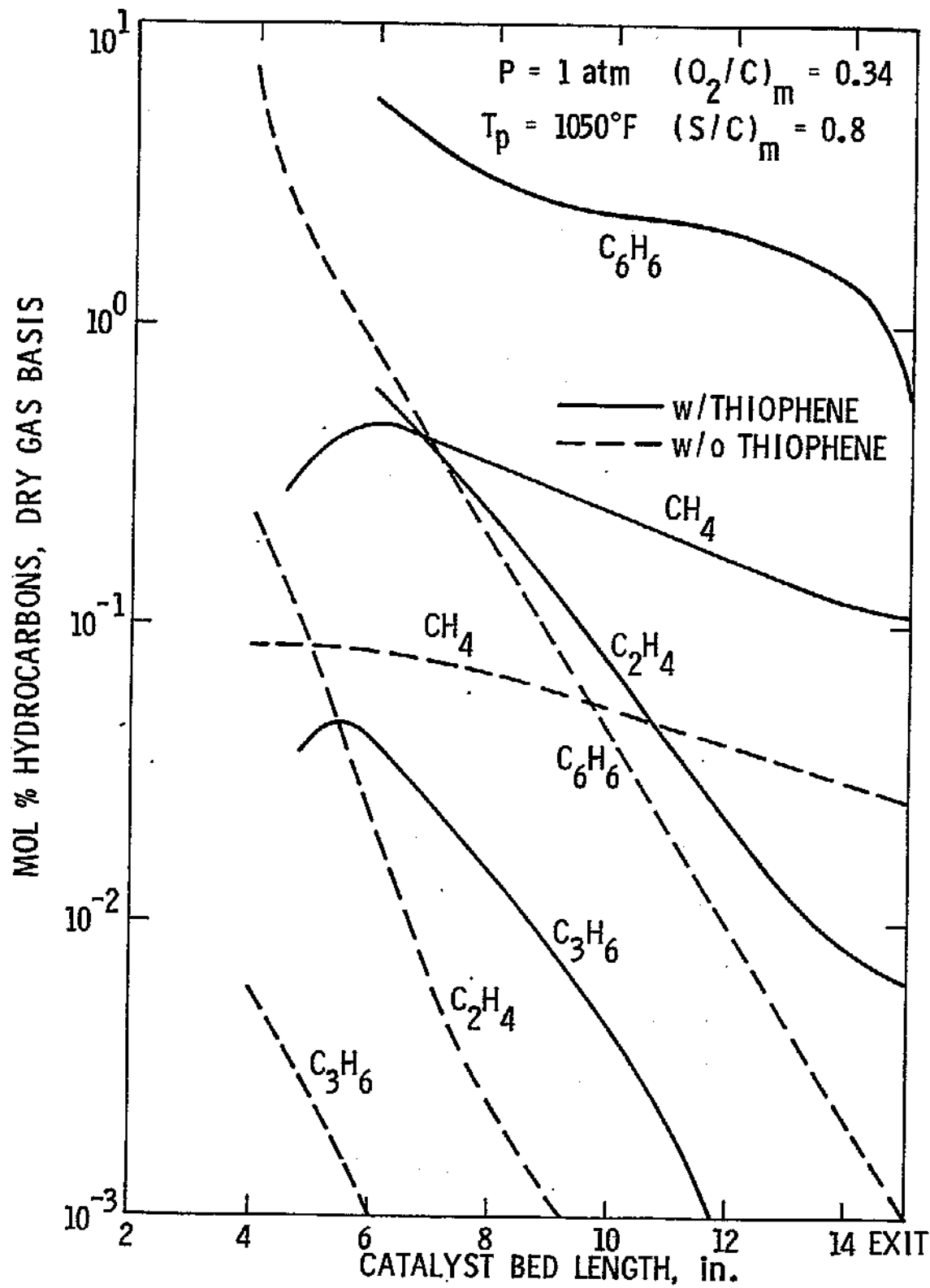


Figure 17. Autothermal Reforming of Benzene, neat and
 with 1750 ppmw Thiophene.
 Axial Bed Composition Profiles.

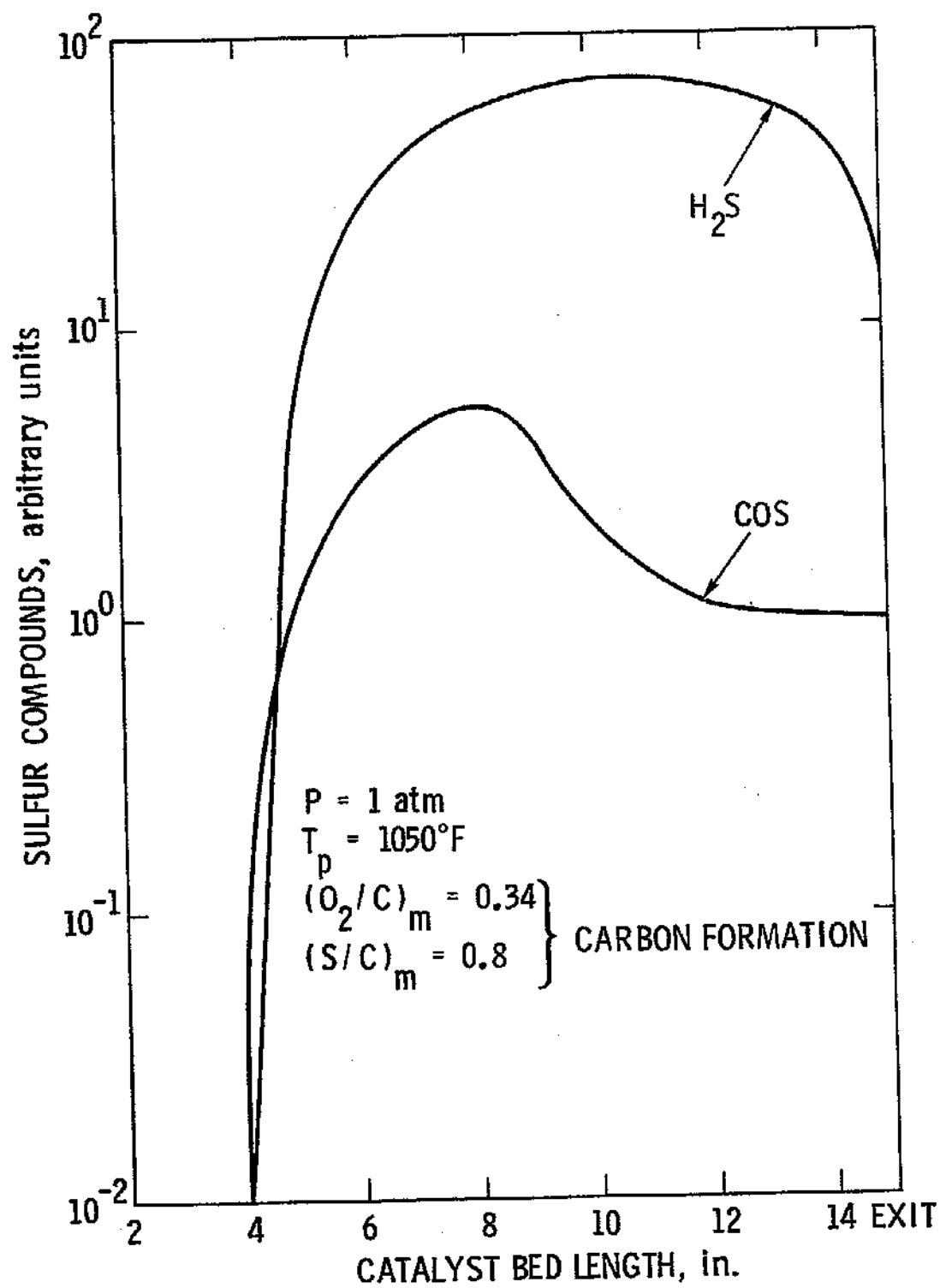


Figure 18. Autothermal Reforming of Benzene with 1750 ppmw Thiophene.
 Gas Phase Axial Profiles of Sulfur Compounds.

Post-examination of the catalysts used at the conditions of Figures 16-18 was performed by SEM/EDAX. All catalyst samples had changed color from gray to green during operation. Sulfur was found on the surface of all three catalyst types, indicating that sulfur had reacted with the catalyst/support throughout the bed. Presumably a sulfate had been formed on the catalyst surface in the partial oxidation region. Figure 19 shows a SEM photomicrograph of the top ICI 46-4 catalyst surface on which crystalline material is seen. This "sulfated" catalyst was less active in ATR than the uncontaminated catalyst.



Figure 19. SEM photomicrograph of the surface of the top ICI 46-4 catalyst used in ATR of the benzene/thiophene mixture at $P = 1 \text{ atm}$, $T_p = 1030^\circ\text{F}$, $(O_2/C)_m = 0.34$, $(S/C)_m = 0.8$, and $S.V. = 9440 \text{ hr}^{-1}$; 2000 X.

CONCLUSIONS

In autothermal reforming work at JPL, a comparative study has been undertaken whereby different types of liquid hydrocarbons, additives, and mixtures thereof have been examined from the aspect of chemical reactivity and carbon formation characteristics in ATR. Effects of changing several of the operating parameters on the propensity for carbon formation have been studied with each hydrocarbon type.

In experiments with sulfur-free hydrocarbon liquids, paraffins and aromatics have been tested extensively in ATR to identify possible reactive differences or similarities that could explain (at least in part) the behavior of heavy fuels, e.g., No.2 fuel oil, which is mainly comprised of paraffins and aromatics. In an earlier experimental study of No.2 fuel oil in ATR (6), this had been found to form carbon at oxygen/steam ratios much higher than those predicted by thermodynamic equilibrium. In the work discussed here, the same catalyst types and configuration have been used as in the fuel oil tests to facilitate comparisons.

Reactive differences between paraffins and aromatics have been found in ATR. These were indicated by very different bed temperature profiles obtained from each fuel type under similar operating conditions. Also, very different experimental carbon formation lines (in the $(O_2/C)_m$ - $(S/C)_m$ plane) were determined for each hydrocarbon. Thus, at low $(S/C)_m$ ratios, paraffins were more prone to form carbon if the $(O_2/C)_m$ ratios were low, while high $(O_2/C)_m$ ratios were unfavorable (carbon-forming) for the aromatics at the same operating conditions.

Gaseous reaction products obtained from different locations throughout the length of the catalyst bed have been analyzed and compared for n-tetradecane (a paraffin) and benzene (an aromatic). Intermediate species (hydrocarbons) identified from each fuel type were different in amounts, not in types. However, the conversion profiles of these intermediates along the bed and the respective bed temperatures profiles are indicative of different carbon formation mechanisms operative for each hydrocarbon type in ATR. In the case of n-tetradecane, considerable cracking to mainly olefinic compounds takes place at the inlet and throughout the partial oxidation region of the bed. These olefins can easily degrade to carbon either in the gas phase (at the higher temperatures, $>1500^{\circ}\text{F}$, close to the temperature peak location), or on the catalyst/support surfaces at high and intermediate temperatures. In the case of benzene, however, no inlet cracking, and very low amounts of olefinic intermediates are produced in the front end of the bed; the predominant species is unconverted benzene throughout the bed. Benzene can degrade to carbon by dehydrogenation in the gas phase at the higher temperatures prevailing in the vicinity of the temperature peak, which is 200°F higher than for n-tetradecane due to the absence of cracking. Benzene-nickel interaction resulting in surface-bound carbon is also possible throughout the steam reforming region of the reactor.

Carbon types and locations of carbon formation were identified for each sulfur-free fuel used in ATR. In all cases, carbon was a mixture of seemingly gas phase generated as well as surface-bound forms. The former was powder-like, filling catalyst voids and not adhering to the surface. The latter was filamentous carbon (whiskers growths) of the kind that has been observed in the steam reforming, CO disproportionation, and methanation literature. As was found by XRD analyses, both types of carbon were (at least in part) graphitic.

With aromatics, gas phase carbon appeared to be the predominant type of carbon in the ICI catalyst zone, which exhibited limited erosion. With paraffins, however, considerable catalyst erosion was typically observed in the ICI zone. Carbon from this part of the bed clearly consisted of a mixture of fines and surface grown whiskers. On the last catalyst zone, G-56B, surface grown carbon was detected regardless of the hydrocarbon type, but considerable catalyst disintegration (fines) was also observed in this zone.

The described characteristics of n-tetradecane and benzene in ATR were the same for their homologs, n-hexane and naphthalene, respectively. The main conclusion here is that the higher the molecular weight, the higher the propensity for carbon formation in ATR. The use of benzene/naphthalene mixtures caused a more pronounced departure from the equilibrium carbon line even at low (<0.36) $(O_2/C)_m$ ratios, indicative of a higher carbon-forming tendency of the polynuclear aromatic molecule (naphthalene).

Intermediate species from either aromatics or paraffins in ATR have been found to vary in amounts only, not in type, when comparing carbon-forming to carbon-free conditions. This probably indicates that a "critical" amount of each carbon precursor (olefinic, aromatic) must be reached in the bed before the local $(S/C)_m$ ratios become too low for carbon-free operation. It was previously (11) shown that the propensity for carbon formation in the steam reforming region of the bed was more sensitive to changes in the local $(S/C)_m$ ratios than to temperature for the same other operating parameters.

Effects of olefin (propylene) addition on the ATR performance of benzene have been described in this report. The "tolerance" of the system (i.e., resistance

to carbon formation) to propylene addition at the inlet is higher than to injections at locations within the steam reforming region of the bed. Propylene addition inhibits the conversion of benzene and enhances methane production in the lower part of the bed. After a "critical" amount of propylene is injected in this region, a reduction in the overall $(S/C)_m$ ratio is effected such that the carbon formation rate becomes faster than that of carbon removal. From these tests, however, it cannot be deduced that propylene itself is the carbon precursor. Higher amounts of unconverted benzene are now present in the bed which may degrade to carbon. To elucidate the mechanism of carbon formation in this case would require well controlled, small scale experiments (e.g., labeling experiments using carbon isotopes).

When mixtures of paraffins and aromatics (n-tetradecane and benzene) were tested in the autothermal reformer under similar conditions as for the pure hydrocarbon components, synergistic effects were identified. Thus, bed temperatures, extent of cracking reactions, and propensity for carbon formation for the mixtures were intermediate between those of the component fuels, n-tetradecane and benzene.

Comparisons of the whole body of experimental ATR results of sulfur-free pure hydrocarbons with No.2 fuel oil (Figure 11) indicate that the deviation of the carbon formation line of the latter from those of the pure hydrocarbon liquids cannot be explained by molecular weight and chemical character (e.g., aromaticity) effects alone. It appears that the sulfur content of No.2 fuel oil (3000-5000 ppmw) may be the limiting factor for an efficient (low O_2/C and preheat temperature) ATR operation. Exploratory tests were thus undertaken in which the effect of sulfur on the conversion characteristics of paraffins

and aromatics in ATR was examined by using mixtures of n-tetradecane and thiophene (2000 ppmw), and benzene and thiophene (1750 ppmw), respectively. Thiophene was chosen as the sulfur additive in these tests, because most of the fuel-bound sulfur in No.2 fuel oil is thiophenic.

Data from the thiophene-containing hydrocarbons were similar for both hydrocarbon types (paraffins, aromatics). Thus, the front part of the bed rapidly became poisoned, and temperature profile peaks were shifted down the bed, while reaction rates were inhibited, as indicated by lower bed temperatures. Upon post-examination of catalyst surfaces from this part of the bed, crystalline material, possibly inorganic sulfates, was detected by SEM, and sulfur was identified by EDAX. The steam reforming region of the bed operated under higher temperatures (since the temperature peak was shifted down the bed). Gas analysis throughout the bed length showed enhanced cracking rates of n-tetradecane, and limited conversion of benzene in the presence of thiophene. These results indicate that carbon formation would take place easier for the sulfur-contaminated than for the sulfur-free fuels, as was actually the case in one set of operating conditions with the benzene/thiophene mixture. Catalyst from the steam reforming region of the bed also contained sulfur, but it was not possible to quantitatively determine if the sulfur-catalyst interaction was lower there than in the partial oxidation region of the bed.

Sulfur species identified by G.C. (FPD) in the gas phase include H_2S (predominantly) and COS apart from unconverted thiophene. However, thiophene was the only sulfur species in the gas phase down to the vicinity of the maximum temperature, where H_2S and COS were first detected. It appears that stable

surface compound(s) formed from the thiophene-catalyst interaction in the upper part of the bed where oxygen is present, since thiophene was being depleted and no other sulfur compound could be detected in the gas phase. On the other hand, the H_2S - nickel interaction in the lower part of the bed appears to be limited, since the H_2S profile is flat through this part. The reason for this may be that higher bed temperatures and sufficient hydrogen pressure there do not favor stable nickel sulfide(s). The sulfur detected (by EDAX) on catalyst samples taken from the lower part of the bed may be due to transients in operation.

These preliminary experimental results from the ATR of sulfur-containing paraffins and aromatics appear to indicate the necessity for higher preheat temperatures in order to alter the thermodynamic equilibrium of the reactions in the front part of the bed and avoid deactivation. This, however, may require increased amounts of steam at the inlet to control potential carbon formation, which can occur from precombustion (in the gas phase) of the fuel at very high inlet temperatures ($\sim 1400^\circ\text{F}$). Future experiments should focus on examining the effects of these parameters (preheat, steam) on the ATR of sulfur-containing hydrocarbons with respect to conversion efficiency and propensity for carbon formation. Based on the outcome of this research, a realistic model can be constructed for the autothermal reforming of fuels of any composition. Moreover, by carefully monitoring all reaction species and apparent catalyst activities in complementary catalyst screening experiments, it will be possible to determine the optimal catalyst types and configurations needed for carbon-free ATR operation under high thermal and conversion efficiencies.